Ideal switched-model dynamic stability conditions for semi-quasi-Z-source inverters☆

Lisandro De Nicoló [a], Hernan Haimovich [a], Richard H. Middleton [b]

[a] CIFASIS-CONICET and Univ. Nac. de Rosario, Ocampo y Esmeralda, 2000 Rosario, Argentina
[b] Centre for Complex Dynamic Systems and Control, The University of Newcastle, Callaghan, NSW 2308, Australia

ARTICLE INFO

ABSTRACT

The ideal switched model of the recently introduced semi-quasi-Z-source inverter is a practical example of a switched system where each subsystem is neither asymptotically stable nor detectable from the output, yet asymptotic stability can be ensured by imposing limitations on the load and on how switching is performed. In this paper, we present novel stability conditions for the switched model (i.e. not the averaged model) of the semi-quasi-Z-source inverter connected to different types of loads and operating in both complementary and uncontrolled conduction. These stability conditions give theoretical justification to the standard open-loop inverter operation strategy and are important for the operation of the converter under closed-loop control.

© 2015 Elsevier Ltd. All rights reserved.

1. Introduction

The semi-quasi-Z-source inverter introduced in Cao, Jiang, Yu, and Peng (2011) is a single-phase single-stage low-cost (only two active components) transformerless inverter whose input and output terminals share the same ground. This inverter is especially suited for renewable-energy distributed-generation photovoltaic applications. Its name derives from the Z-source inverter (Peng, 2003; Tang, Xie, & Zhang, 2011) because it also contains an LC network, the distinguishing feature of the Z-source inverter. However, the shoot-through state responsible for the boost capability of the Z-source inverter does not apply to the semi-quasi-Z-source inverter and hence the principle of operation of the latter inverter is substantially different. The semi-quasi-Z-source inverter is depicted in Fig. 1. This inverter contains two active components (such as IGBTs or MOSFETs), named S_1 and S_2 in Fig. 1. These components conduct in a complementary manner during normal operation, i.e.

either S_1 is on and S_2 is off, or S_1 is off and S_2 is on. We refer to this "normal" operation mode as *complementary conduction* mode (CCM). By *uncontrolled conduction* mode (UCM) we refer to the situation when both S_1 and S_2 are on because the antiparallel diode of the non-triggered transistor becomes forward biased. Standard operation of the inverter involves generating the gate signal for each transistor via pulse-width modulation (PWM) so that exactly only one of the transistors is triggered at every time instant. The fraction of the PWM carrier period that S_1 is on is referred to as the duty cycle of S_1. In CCM, if the duty cycle of S_1 is d, then that of S_2 will be $1 - d$.

To obtain a sinusoidal voltage waveform at the output of the inverter, Cao et al. (2011) assert that if the frequency of the desired output sine wave is low enough, then the steady-state averaged-model input–output gain equation would be approximately valid at every time instant (after a possible initial transient). Hence the required time-varying duty cycle can be deduced from this gain equation. This inverter operation strategy was successfully tested on a 40W prototype connected to a linear purely resistive load. Operating the inverter in this manner necessarily produces large-signal behavior, meaning that the linearized averaged model (Ćuk, 1977; Erickson, Ćuk, & Middlebrook, 1982; Middlebrook & Ćuk, 1976) is not an accurate model of the evolution of the circuit variables.

The fact that the operation strategy proposed by Cao et al. (2011) showed acceptable results when tested on the experimental prototype motivates the study of several important issues that have not been previously analyzed. These issues involve the

Fig. 1. Semi-quasi-Z-source inverter.

determination of whether different initial conditions converge to the same steady-state trajectory or whether the state trajectory remains bounded from every practical initial condition. Moreover, it would be very useful to understand whether the transient occurrence of UCM can alter the steady-state or the asymptotic behavior. The importance of these issues is not only theoretical but also practical, since specific types of loads, duty cycle evolutions, and switching frequencies may lead to instability and the occurrence of UCM, as we will demonstrate by means of two simulation examples in Section 2.

Previous work in relation to the aforementioned issues in the semi-quasi-Z-source inverter has been presented in De Nicoló, Haimovich, and Middleton (2013) and Haimovich, Middleton, and De Nicoló (2013). In Haimovich et al. (2013), we presented large-signal stability conditions for both the averaged and the switched model of the inverter connected to a purely resistive linear load and operating in CCM. For both models, we showed that (a) the state trajectories remain bounded irrespective of the (time-varying) duty cycle evolution and (b) the state trajectories corresponding to the same duty cycle evolution but starting from different initial conditions converge to the same steady-state trajectory. These results hold provided reasonable operating conditions are satisfied. For the averaged model, these conditions amount to keeping the duty cycle away from the extreme values 0 or 1. For the switched model, in addition, the PWM carrier period must be less than a specific value. In De Nicoló et al. (2013), we extended these stability results to the switched model of the inverter connected to a purely resistive but nonlinear load.

This work extends the switched-model stability results of De Nicoló et al. (2013) and Haimovich et al. (2013) in several directions. First, we provide simulation examples to illustrate the behavior of the semi-quasi-Z-source inverter and single out the precise mechanism responsible for the generation of instability. Second, we give stability conditions for specific types of nonlinear dynamic and time-varying loads. Third, we enlarge the class of considered switching signals so that our results hold for every switching signal that ensures a minimum dwell-time on each mode and an upper bound on the time spent in two consecutive modes. This class contains but is not limited to the signals corresponding to PWM operation. Fourth, stability results that include possible transient occurrence of UCM are established. Our results contain the switched-model results of De Nicoló et al. (2013) and Haimovich et al. (2013) as special cases.

Standard results on open-loop trajectory stability based on switched models and for a broad class of converters are presented in Sanders and Verghese (1992). These results show that the difference between trajectories that correspond to the same switching evolution but different initial conditions is always bounded. To conclude that this difference will asymptotically converge to zero, Sanders and Verghese (1992) require the existence of parasitic loss associated to each storage element of the circuit. By contrast, the asymptotic and exponential stability results that we provide regard all active and passive components in the inverter circuit as ideal components. These assumptions correspond to a converter with 100% energy efficiency. Our results thus show that open-loop stability of the semi-quasi-Z-source inverter does not require parasitic

losses. As noted in Sanders and Verghese (1992), energy dissipation within the converter circuit is helpful towards achieving stability.

Most existing results on switching converter stability either are based on an averaged model of the circuit or address only closed-loop operation. The use of averaged models for stability analysis is known to give rise to switching frequency-dependent mismatch between predicted and observed behavior, especially in closed-loop operation (Lehman & Bass, 1996). Open-loop stability of the semi-quasi-Z-source inverter based on the switched model (i.e. not the averaged model) becomes important because, as opposed to other topologies, this specific inverter circuit may exhibit some singular unstable trajectories that should be avoided (see Section 2.5). A similar problem exists in the Ćuk converter, (see, e.g., Fuad, de Koning, & van der Woude, 2004).

A key difficulty in the analysis of the semi-quasi-Z-source inverter is that neither of the switching modes (neither of the subsystems, employing switched systems terminology Liberzon, 2003) is asymptotically stable nor detectable from the output voltage, and hence stability is dependent on the limitations imposed on switching. In addition, since neither mode is asymptotically stable, then a minimum dwell-time condition is not sufficient in order to ensure asymptotic stability. Therefore, some available switched-system extensions of LaSalle's invariance principle (Bacciotti & Mazzi, 2005; Cheng, Wang, & Hu, 2008; Hespanha, 2004) are not applicable or do not yield useful information when applied to the switched model of the semi-quasi-Z-source inverter.

In Section 2 we present the switched model of the semi-quasi-Z-source inverter and the specific types of loads and switching signals that we may consider. We also briefly explain the operation strategy proposed in Cao et al. (2011) and provide motivating simulation examples where instability is evidenced. Section 3 contains stability results for the inverter operating in CCM and Section 4 those that consider the occurrence of UCM. Conclusions are given in Section 5. Most proofs are given in the Appendix.

Notation. The reals, nonnegative reals, and integers are denoted $\mathbb{R}$, $\mathbb{R}_+$, and $\mathbb{Z}$, respectively. For a matrix M, $\rho(M)$ denotes its spectral radius, M' its transpose, and $M > 0$ means that M is positive definite. The ith column of the identity matrix is e_i and $\|\cdot\|$ denotes the (induced) 2-norm.

2. Semi-quasi-Z-source inverter

The semi-quasi-Z-source inverter is depicted in Fig. 1. In CCM, either S_1 is on and S_2 is off (Mode I) or S_1 is off and S_2 is on (Mode II). In UCM a third mode (Mode III) occurs when the switches S_1 and S_2 are both conducting. The inverter reaches Mode III when operating in Mode I and the antiparallel diode of S_2 becomes forward biased, or when operating in Mode II and that of S_1 becomes forward biased.

The switched model of the inverter operating in CCM is presented in Section 2.1. In Sections 2.2 and 2.3, we describe the types of switching signals and loads, respectively, considered. In Section 2.4, we briefly explain the inverter operation strategy proposed by Cao et al. (2011). In Section 2.5, we illustrate the possible unstable behavior of the inverter by means of simulation examples.

2.1. Switched model in CCM

Consider the semi-quasi-Z-source inverter of Fig. 1. Defining the state vector z_c as,

$$z_c := [i_{L_1} i_{L_2} v_{C_1} v_{C_2}]',\tag{1}$$

with the positive convention for each variable as shown in Fig. 1, the state equation for the switched model of the inverter in CCM

can be written as

$$P_c \dot{z}_c(t) = [A_\text{I}^q z_c(t) + b_\text{I}^q] r(t) + [A_\text{II}^q z_c(t) + b_\text{II}^q][1 - r(t)] - e_4 i_o \quad (2)$$

$$A_\text{I}^q = \begin{bmatrix} 0 & 0 & 0 & 0 \\ 0 & 0 & 1 & 1 \\ 0 & -1 & 0 & 0 \\ 0 & -1 & 0 & 0 \end{bmatrix}, \qquad A_\text{II}^q = \begin{bmatrix} 0 & 0 & -1 & 0 \\ 0 & 0 & 0 & 1 \\ 1 & 0 & 0 & 0 \\ 0 & -1 & 0 & 0 \end{bmatrix}, \quad (3)$$

$$b_\text{I}^q = \begin{bmatrix} V_\text{in} & 0 & 0 & 0 \end{bmatrix}', \qquad b_\text{II}^q = \begin{bmatrix} 0 & -V_\text{in} & 0 & 0 \end{bmatrix}', \quad (4)$$

$$P_c := \text{diag}(L_1, L_2, C_1, C_2), \quad v_o = z_{c_4} = e_4' z_c, \quad (5)$$

$$r(t) = \begin{cases} 1 & \text{if in Mode I}, \\ 0 & \text{if in Mode II}, \end{cases} \quad (6)$$

where $e_4 = [0\ 0\ 0\ 1]'$ and i_o denotes the current drawn by the load (i.e. the inverter's output current), whose positive convention is shown in Fig. 1. The signal $r : \mathbb{R}_+ \to \{0, 1\}$ is the *switching signal*, whose value $r(t)$ identifies which of the modes is active at instant t.

2.2. Switching signals

We will consider switching signals in the following class.

Definition 1. A signal $r : \mathbb{R}_+ \to \{a, b\}$, with $a \neq b$, is said to be of class $\overline{\mathbb{PWM}}(T, \epsilon)$ with $0 < 2\epsilon \leq T$, if it is right-continuous and for every integer k there exist time instants τ_k and r_k, so that $r_0 = 0$ and

$$r(t) = \begin{cases} a & \text{if } r_k \leq t < \tau_k, \\ b & \text{if } \tau_k \leq t < r_{k+1}, \end{cases} \quad (7)$$

$$\tau_k - r_k \geq \epsilon, \qquad r_{k+1} - r_k \leq T, \quad (8)$$

$$r_{k+1} - \tau_k \geq \epsilon.$$

A signal of class $\overline{\mathbb{PWM}}(T, \epsilon)$ is said to be of class $\mathbb{PWM}(T, \epsilon)$ if the time instants r_k satisfy $r_{k+1} - r_k = T$.

A signal r of class $\overline{\mathbb{PWM}}(T, \epsilon)$ constantly alternates between its two possible values (modes) a and b. According to (7), the time instants r_k and τ_k are the discontinuity instants of r, and from (8) then each mode has minimum and maximum dwell-times ϵ and $T - \epsilon$, respectively. The output of a PWM with carrier period equal to T and where the duty cycle of either mode is never less than ϵ/T is a signal of class $\mathbb{PWM}(T, \epsilon) \subset \overline{\mathbb{PWM}}(T, \epsilon)$.

2.3. Loads

We consider loads described in one of the forms:

$$\text{PHF} \begin{cases} \dot{x}_l = [J - R(t, x_l)] P_H x_l + B v_o \\ i_o = [B + K]' P_H x_l + h(t, v_o) \end{cases} \quad (9a)$$

$$\text{PH} \begin{cases} \dot{x}_l = [J - R(t, x_l)] P_H x_l + B v_o \\ i_o = B' P_H x_l \end{cases} \quad (9b)$$

$$\text{TVS} \begin{cases} i_o = h(t, v_o) \end{cases} \quad (9c)$$

where $R(t, x_l)$ and $h(t, v_o)$ are continuous and

$$J = -J', \qquad P_H = P_H' > 0, \quad (10)$$

$$R(t, x_l) = R'(t, x_l) > 0, \quad \forall t, \ \forall x_l.$$

A load of the form (9a) is a time-varying nonlinear load that can be interpreted as a port-Hamiltonian system with feedthrough (PHF), where J is the interconnection matrix, $R(t, x_l)$ is the dissipation matrix, $h(t, v_o)$ is the *feedthrough* term, and where the Hamiltonian is quadratic and given by $H(x_l) = \frac{1}{2} x_l' P_H x_l$. A load of the form (9b) lacks the feedthrough term and one of the form (9c) is a time-varying static (TVS) nonlinearity. Note that both (9b) and (9c) are special cases of (9a). We will impose the following assumptions on the load.

- For a PHF load (9a):

$$h_m v_o^2 \leq v_o h(t, v_o) \leq h_M v_o^2, \qquad \forall t, \forall v_o, \quad (11)$$

$$\lambda_m I \leq R(t, x_l) - \frac{KK'}{4h_m} \leq \lambda_M I, \qquad \forall t, \forall x_l, \quad (12)$$

with $R(t, x_l)$ and $h(t, v_o)$ continuous and with positive constants $h_M \geq h_m > 0$ and $\lambda_M \geq \lambda_m > 0$.

- For a PH load (9b):

$$\lambda_m I \leq R(t, x_l) \leq \lambda_M I, \qquad \forall t, \forall x_l, \quad (13)$$

with $R(t, x_l)$ continuous and $\lambda_M \geq \lambda_m > 0$.

- For a TVS load (9c), only (11) will be required, with $h(t, v_o)$ continuous and $h_M \geq h_m > 0$.

The use of a port-Hamiltonian description in switched converters was analyzed in Escobar, van der Schaft, and Ortega (1999). The form (9) allows the modeling of loads that can be thought of as RLC circuits with possibly nonlinear time-varying resistors. Loads that are not covered by our current analysis include those having nonlinear energy-storage components, such as a nonlinear inductor. Note that a linear resistive load of equation $i_o = G v_o$, with conductance $G > 0$, is a special case of (9c), and satisfies (11) with $h_m = h_M = G$. Another important type of load that can be put into one of the forms (9) is the following.

Proposition 1. *Consider a linear load of admittance*

$$Y(s) = \frac{I_o(s)}{V_o(s)},$$

where $I_o(s)$ and $V_o(s)$ represent the Laplace transforms of the load current and voltage, respectively. If $Y(s)$ is strictly positive real (SPR), then the load's state and output equations can be put into one of the forms (9), satisfying the corresponding assumptions in (11), (12), (13). ○

The proof of Proposition 1 is based on the Kalman–Yakubovich–Popov Lemma (cf. Khalil, 2002, Lemma 6.3) and is omitted due to space limitations.

2.4. Standard open-loop operation

The DC gain equation for the semi-quasi-Z-source inverter is derived in Cao et al. (2011) as

$$\frac{\overline{\langle v_o \rangle}}{V_\text{in}} = \frac{\overline{\langle v_{C_2} \rangle}}{V_\text{in}} = \frac{1 - 2D}{1 - D}, \quad (14)$$

where $\overline{\langle y \rangle}$ denotes the average value of y over a switching period and D is the constant duty cycle of Mode I. Cao et al. (2011) state that if a time-varying duty cycle is applied with a sufficiently slow variation, then (14) would be approximately valid at every time instant. Consequently, if $\langle v_o(t) \rangle = V_o \sin(2\pi f_o t)$ is desired, then from (14), the required time-varying duty-cycle $d(t)$ results

$$d(t) = \frac{1 - M \sin(2\pi f_o t)}{2 - M \sin(2\pi f_o t)} \quad (15)$$

with $M = \frac{V_o}{V_\text{in}}$. Cao et al. tested this inverter operation strategy on a 40 W prototype showing good results when the inverter is connected to a linear resistive load.

2.5. Unstable/UCM trajectory examples

We next present two simulation examples. The first simulation corresponds to the inverter connected to a linear resistive load.

Capacitor C_1 voltage

Capacitor C_2 voltage
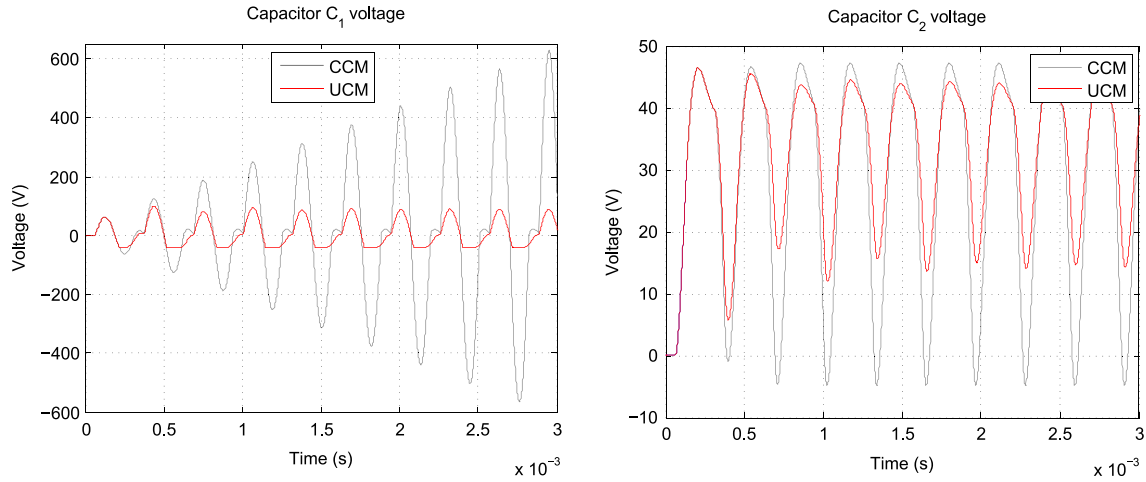
Fig. 2. Capacitor C_1 voltage and capacitor C_2 voltage. (For interpretation of the references to color in this figure legend, the reader is referred to the web version of this article.)

The values of inductance, capacitance, input voltage, and load resistance are taken to coincide with those of the 40W prototype of Cao et al. (2011). That is, $L_1 = L_2 = 400\,\mu\mathrm{H}$, $C_1 = C_2 = 4\,\mu\mathrm{F}$, $V_{\mathrm{in}} = 40\,\mathrm{V}$, $R = 19\,\Omega$. Initial conditions for the simulation are 1 mA for the inductor L_1 current and zero for the rest of the state variables. The switching signal $r(t)$ is given by

$$r(t) = \begin{cases} 1 & \text{if} \quad d(t) > p(t), \\ 0 & \text{if} \quad d(t) \le p(t), \end{cases} \tag{16}$$

$$p(t) = \frac{t}{T} - k(t), \quad k(t) = \text{floor}\left(\frac{t}{T}\right), \tag{17}$$

where floor(a) denotes the greatest integer not greater than a, $T = 2.5\pi\sqrt{L_1 C_1} = 314\,\mu\mathrm{s}$, and $d(t) = 0.2$ (constant). The generation of $r(t)$ in this manner is nothing but a pulse-width modulation of the signal $d(t)$. The signal $d(t)$ can be interpreted as the required duty cycle of Mode I, which is compared with the sawtooth signal $p(t)$ to generate the switching function $r(t)$. Since the duty cycle of Mode I is constant, then according to the steady-state equation (14) the average value of the output voltage would be 30V. Note that $r(t)$ as above is of class $\mathbb{PWM}(T, \epsilon)$ with $\epsilon = 0.2T$. Fig. 2 shows the capacitors C_1 and C_2 voltage, in red when UCM occurrence is considered and in black if UCM did not occur. For the inverter to remain in CCM, the instantaneous voltage across C_1 has to remain greater than $-V_{\mathrm{in}}$, i.e. $v_{C_1}(t) > -V_{\mathrm{in}}$. This is required to ensure that neither the antiparallel diode of S_2 (if in Mode I) nor that of S_1 (if in Mode II) becomes forward biased. This example shows that although the inverter is connected to a linear resistive load (the same load used by Cao et al. (2011) in the 40 W prototype) and the duty cycle of Mode I is constant and equal to 0.2, the state trajectory would diverge if UCM did not occur. The corresponding averaged model is stable in this case (see Haimovich et al., 2013) and hence this simulation example shows the need of considering a switched model in order to properly analyze stability.

The second simulation corresponds to a purely resistive nonlinear load with current–voltage relationship

$$i_o = 0.5\,\text{sat}(2v_o/R), \qquad R = 19\Omega, \quad \text{where} \tag{18}$$

sat$(\cdot)$ is the standard saturation function. This load behaves as a linear resistive load of resistance $R = 19\Omega$ if the absolute value of its voltage is less than 9.5 V; otherwise, it draws a constant current of 0.5 A or -0.5 A. Note that the relationship (18) satisfies $v_o h(t, v_o) \ge 0 \;\forall v_o \in \mathbb{R}$ and $\forall t$ with $h(t, v_o) := 0.5\,\text{sat}(2v_o/R)$. Parameter values are taken to coincide with those of the 40 W prototype in Cao et al. (2011). That is, $L_1 = L_2 = 400\,\mu\mathrm{H}$, $C_1 = C_2 = 4\,\mu\mathrm{F}$, $V_{\mathrm{in}} = 40\,\mathrm{V}$. The load behaves identically to that in

the aforementioned prototype if the absolute value of the output voltage is less than 9.5V.

The aim of this second simulation example is to illustrate the fact that even if the load is strictly passive and the duty cycle never deviates much from 0.5, some duty cycle evolutions may still cause instability. Bearing this aim in mind, we consider a switching signal defined by (16)–(17), and with $d(t)$ as below, which is purposely selected in order to generate instability:

$$d(t) = 0.5 + 0.028 \,\text{sign}\left[i_{L_1}\big(k(t)T\big) + i_{L_2}\big(k(t)T\big)\right].$$

The sawtooth signal period T (PWM carrier period) is now selected equal to that used for the aforementioned prototype, namely $T = 20\,\mu\mathrm{s}$, corresponding to a switching frequency of 50 kHz. The simulation was run with zero initial conditions in all state variables. Again, note that the switching signal $r(t)$ for this second simulation example is of class $\mathbb{PWM}(T, \epsilon)$ with period $T = 20\,\mu\mathrm{s}$ and minimum dwell-time $\epsilon = (0.5 - 0.028)T = 0.472\,T$. Fig. 3 shows the simulation results until $t = 0.09$ s. Fig. 3 exhibits the occurrence of UCM (Mode III), when $v_{C_1}(t)$ reaches $-V_{\mathrm{in}}$. In this example, the time-varying duty cycle applied assumes only the two values $0.5 - 0.028 = 0.472$ and $0.5 + 0.028 = 0.528$. Also, note that the inverter is connected to a passive non-linear resistive load ($v_o i_o$ is always nonnegative). Despite these facts, and that the switching frequency is high (50 kHz), the state trajectory would diverge if UCM did not occur.

The mechanism for instability is different in each simulation example. In the first example, some of the energy delivered by the voltage source is stored in L_1 and C_1 and never reaches the rest of the circuit. This is evidenced in Fig. 2 by the fact that the capacitor C_1 voltage diverges if UCM did not occur, but not the capacitor C_2 voltage. This type of instability occurs because the switching frequency is not sufficiently high. The second example shows that even if the switching frequency is sufficiently high and the energy contained in L_1 and C_1 can be transferred to the rest of the circuit, the rate at which the load dissipates energy eventually becomes lower than the rate at which the input voltage source delivers energy to the circuit, causing all variables to become divergent if UCM did not occur.

3. Complementary Conduction Mode (CCM)

In this section, we provide stability results for the switched model of the semi-quasi-Z-source inverter operating in CCM. For simplicity of the resulting equations, we will express the state equations in the variables

$$x_c(t) := z_c(t) - \bar{z}_c, \qquad\qquad \mu(t) := r(t) - 0.5, \tag{19}$$
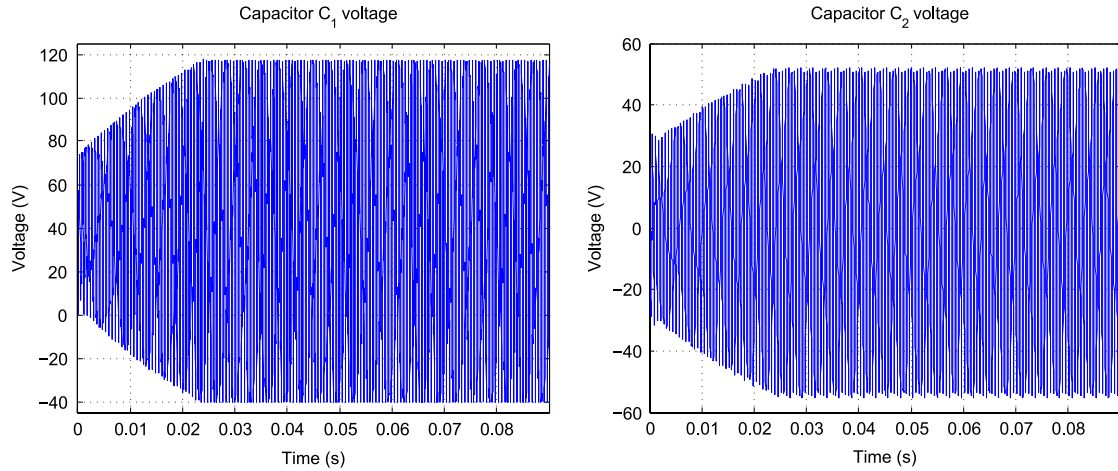
Fig. 3. Capacitor C_1 and C_2 (output) voltages.

with $\bar{z}_c = [0 \ 0 \ V_{\text{in}} \ 0]'$. In terms of x_c and μ, the switched model (2)–(6) becomes

$$\dot{x}_c(t) = A_c(\mu(t))x_c(t) + B_c i_o + B_{\text{in}}\mu(t), \text{ where} \quad (20)$$

$$A_c(\mu(t)) = P_c^{-1}\left[A_0^q + E_0^q\mu(t)\right], \quad (21)$$

$$B_{\text{in}} = P_c^{-1}[2V_{\text{in}} \ 2V_{\text{in}} \ 0 \ 0]', \qquad B_c = -P_c^{-1}e_4 \quad (22)$$

$$A_0^q = \begin{bmatrix} 0 & 0 & -0.5 & 0 \\ 0 & 0 & 0.5 & 1 \\ 0.5 & -0.5 & 0 & 0 \\ 0 & -1 & 0 & 0 \end{bmatrix}, \quad E_0^q = \begin{bmatrix} 0 & 0 & 1 & 0 \\ 0 & 0 & 1 & 0 \\ -1 & -1 & 0 & 0 \\ 0 & 0 & 0 & 0 \end{bmatrix}, \quad (23)$$

with P_c as in (5) and $v_o = e_4'x_c$. According to (19) and since $r(t) \in \{0, 1\}$, then $\mu(t) \in \{-0.5, 0.5\}$. Note that $A_c(-0.5) = P_c^{-1}A_{\text{II}}^q$ and $A_c(0.5) = P_c^{-1}A_{\text{I}}^q$.

The state equations for the connection of a load to the semi-quasi-Z-source inverter are obtained by combining the load equations (9) with the inverter equations (20). This combination can be written as

$$\dot{x}(t) = A(\mu(t))x(t) + F(t, x(t)) + B_s\mu(t), \quad (24)$$

where x is the complete circuit state, $A(\mu)x$ represents a switched-linear part and $F(t, x)$ concentrates nonlinearities, where:

- If the load is of the form PHF, as in (9a), then

$$A(\mu) = \begin{bmatrix} A_c(\mu) + B_c h_m e_4' & B_c[B+K]'P_H \\ Be_4' & A_l \end{bmatrix}, \quad (25)$$

$$x := \begin{bmatrix} x_c \\ x_l \end{bmatrix}, \qquad B_s := \begin{bmatrix} B_{\text{in}} \\ 0 \end{bmatrix}, \quad (26)$$

$$A_l := \left(J - \frac{KK'}{4h_m} - \lambda_m I\right)P_H, \quad (27)$$

$$F(t, x) := \begin{bmatrix} B_c\rho(t, e_4'x_c) \\ -\delta(t, x_l)P_H x_l \end{bmatrix}, \quad (28)$$

$$\delta(t, x_l) := R(t, x_l) - \frac{KK'}{4h_m} - \lambda_m I, \quad (29)$$

$$\rho(t, v) := h(t, v) - h_m v. \quad (30)$$

- If the load is PH, as in (9b), then (25)–(26) hold with $K := 0$ and $h_m := 0$, and (27)–(29) hold with $K := 0$ and $\rho := 0$.
- If the load is TVS, as in (9c), then ρ is as in (30),

$$x := x_c, \qquad B_s := B_{\text{in}}, \qquad F(t, x) := B_c\rho(t, e_4'x_c),$$

$$A(\mu) := A_c(\mu) + B_c h_m e_4'. \quad (31)$$

If the input voltage is time-varying, of the form $v_{\text{in}}(t) = V_{\text{in}}\vartheta(t)$, then the model (24) is written as

$$\dot{x}(t) = A(\mu(t))x(t) + F(t, x(t)) + B_s u(t), \quad (32)$$

where $u(t) = \vartheta(t)\mu(t)$. This follows from (22) and (26). The constant V_{in} now identifies the "nominal" input voltage. Since it is both reasonable and practical to assume that the input voltage is bounded, and since $\mu(t) \in \{-0.5, 0.5\}$, it follows that $u(t)$ bounded is a reasonable and practical assumption. Also, since for constant and nominal input voltage we have $u(t) = \mu(t)$, then $u(t)$ cannot be assumed continuous. Solutions to (32) are understood in the sense of Carathéodory, i.e. absolutely continuous functions $x(t)$ whose time derivative satisfies (32) almost everywhere. For future reference, define

$$A_{\text{I}} := A(0.5), \qquad A_{\text{II}} := A(-0.5), \quad (33)$$

$$P := \begin{cases} \begin{bmatrix} P_c/2 & 0 \\ 0 & P_H/2 \end{bmatrix} & \text{for PHF or PH load,} \\ P_c/2 & \text{for TVS load,} \end{cases} \quad (34)$$

with P_c and P_H as in (5) and (9)–(10).

The following lemma is the starting point for our stability results and constitutes an extension to linear dynamic loads of Lemma 1 of Haimovich et al. (2013). The latter result dealt only with loads of the form $i_o = v_o/R$, with constant R. The proof of Lemma 1 can be consulted in the Appendix.

Lemma 1. *Consider A_{I}, A_{II} and P as in (33)–(34). Let t_{I}, t_{II} be positive and for every $\epsilon \geq 0$ define*

$$M_\epsilon := e^{A_{\text{I}}\epsilon} e^{A_{\text{II}}t_{\text{II}}} e^{A_{\text{I}}t_{\text{I}}}. \quad (35)$$

(a) *If $t_{\text{II}} \neq k\pi\sqrt{L_1 C_1}$ for every positive integer k, then $\rho(M_0) < 1$ and*

$$M_\epsilon' P M_\epsilon - P < 0, \quad \text{for all } \epsilon > 0. \quad (36)$$

(b) *If $t_{\text{II}} = k\pi\sqrt{L_1 C_1}$ for some positive integer k, then $\rho(M_\epsilon) = 1$ for all $\epsilon \geq 0$.*∘

Lemma 1 identifies a key property of the ideal semi-quasi-Z-source inverter circuit. The linear (time-varying) system $\dot{x} = A(\mu)x$ represents the inverter under $V_{\text{in}} = 0$ when connected to a linear load. Recalling (33), we see that A_{I} and A_{II} are the two possible values of $A(\mu(t))$. Given an initial state x_o, the quantity $M_\epsilon x_o$, with M_ϵ as in (35), represents the state that is reached from x_o after operating in Mode I (i.e. $\mu(t) = 0.5$) for t_{I} seconds, followed by Mode II ($\mu(t) = -0.5$) for t_{II} seconds, and again Mode I for ϵ seconds. The

expression $x_o'(M_\epsilon' P M_\epsilon - P)x_o$ constitutes the increment in energy from the initial state x_o to the final state $M_\epsilon x_o$. The main point in Lemma 1 is that if the time spent in Mode II, namely t_{II}, is an integer multiple of $\pi\sqrt{L_1 C_1}$, then initial states will exist from which the system's energy will not decrease, even if we alternate between Modes I and II. This situation may become a stability problem when $V_{in} \neq 0$. This problem is the one illustrated in the first simulation example in Section 2.5. The result of Lemma 1, is directly related to the characterization of observability for switched linear systems given in Tanwani, Shim, and Liberzon (2013), where individual subsystems may be not detectable but detectability of the switched system can still be ensured depending on the mode sequence and switching times. Our main stability result for CCM follows.

Theorem 1. *Consider the system* (32), *representing the ideal switched model of the semi-quasi-Z-source inverter connected to a load of one of the considered forms, as explained in Section* 2.3, *and allowing input voltage variations through the bounded and piecewise continuous perturbation input u. Let ϵ and T satisfy $0 < 2\epsilon \leq T \leq \pi\sqrt{L_1 C_1}$. Then, there exist positive constants $\bar{K}$, λ and G such that the trajectories of* (32) *(i.e. the Carathéodory solutions) are defined for all $t \geq 0$ and satisfy*

$$\|x(t)\| \leq \bar{K}\|x_0\|e^{-\lambda t} + G \sup_{0 \leq \tau \leq t} \|u(\tau)\|, \tag{37}$$

for all $\mu \in \overline{\mathbb{PWM}}(T, \epsilon)$, for all initial state x_0 and all $t \geq 0$. If, in addition, the continuous functions $R(t, x_l)$ and/or $h(t, x_l)$, depending on the load type, are such that $F(t, x)$ in (28)–(30) *is locally Lipschitz in x for all $t \geq 0$, then the solutions $x(t)$ are unique.* ○

Theorem 1 states that system (32) is input-to-state stable with respect to the input $u(t)$, uniformly over switching signals of class $\overline{\mathbb{PWM}}(T, \epsilon)$. Eq. (32) represents the inverter connected to a possibly nonlinear and time-varying dynamic load and under, input voltage variations. The constraint $0 < 2\epsilon \leq T \leq \pi\sqrt{L_1 C_1}$ implies a maximum dwell-time $T - \epsilon \leq \pi\sqrt{L_1 C_1} - \epsilon$. The proof of Theorem 1 is given in the Appendix.

For the specific case of the semi-quasi-Z-source inverter commanded by the output of a PWM with carrier period equal to T, i.e. with switching signal of class $\mathbb{PWM}(T, \epsilon)$, it happens that if the switching frequency is not higher than $1/(\pi\sqrt{L_1 C_1})$, then the time spent in Mode II may equal or approximate $\pi\sqrt{L_1 C_1}$ (or an integer multiple of it). In this case, the circuit variables will not only have large ripple but ripple may also increase without bound, or at least until UCM occurs, as illustrated in the first simulation example in Section 2.5.

The assumptions on the load, as given in Section 2.3, ensure that the load is strictly passive. If the requirement that the load be strictly passive is relaxed to only passive, then the inverter may fail to achieve stability. This can be readily verified by considering a load consisting only of a linear inductor of inductance $L > 0$. The admittance function in this case is $Y(s) = 1/Ls$, which is positive real but not strictly positive real (and hence not strictly passive). Note that in this case, and since we consider all circuit components to be ideal, no energy-dissipating components are present, and hence stability cannot be expected in open loop.

The following theorem can be employed to give theoretical justification to the open-loop inverter operation strategy of Cao et al. (2011) that was explained in Section 2.4.

Theorem 2. *Consider the system* (32), *representing the ideal switched model of the semi-quasi-Z-source inverter connected to a load of one of the considered forms, as explained in Section* 2.3, *and under input voltage variations. Consider the following assumptions on the load:*

- *If the load is PHF, suppose that,*

$$0 < h_m \leq \frac{h(t, v_1) - h(t, v_2)}{v_1 - v_2} \leq h_M, \tag{38}$$

$$\left\|\tilde{\delta}(t, x_l, \varepsilon_l)\right\|^2 \leq a \|P_H \varepsilon_l\|^2, \tag{39}$$

$$\tilde{\delta}(t, x_l, \varepsilon_l)' P_H \varepsilon_l \geq 0, \tag{40}$$

for some $a > 0$, for all $v_1 \neq v_2$, and all t, x_l and ε_l, where

$$\tilde{\delta}(t, x_l, \varepsilon_l) := [R(t, x_l + \varepsilon_l) - R(t, x_l)] P_H x_l$$
$$+ \left[R(t, x_l + \varepsilon_l) - \frac{KK'}{4h_m} - \lambda_m I\right] P_H \varepsilon_l. \tag{41}$$

- *If the load is PH, as in* (9b), *suppose that* (39)–(41) *hold with $K := 0$.*
- *If the load is TVS, as in* (9c), *suppose that* (38) *holds.*

Let ϵ and T satisfy $0 < 2\epsilon \leq T \leq \pi\sqrt{L_1 C_1}$ and let $x^{\mu,u}(t, x_o)$ denote a solution to (32) *at time t, corresponding to the initial condition x_o, switching signal μ, and bounded piecewise continuous perturbation u. Then,*

(a) *if $\mu \in \overline{\mathbb{PWM}}(T, \epsilon)$, and $u(t)$ is bounded and piecewise continuous, then a (Carathéodory) solution $x^{\mu,u}(t, x_o)$ exists for all $t \geq 0$ and is unique.*
(b) *there exist positive constants $\bar{K}$ and λ such that*

$$\|x^{\mu,u}(t, x_{10}) - x^{\mu,u}(t, x_{20})\| \leq \bar{K}e^{-\lambda t}\|x_{10} - x_{20}\| \tag{42}$$

for all $t \geq 0$, all x_{10}, x_{20} and all $\mu \in \overline{\mathbb{PWM}}(T, \epsilon)$. ○

The proof of Theorem 2 is given in the Appendix.

Theorem 2 states that the difference between any two state trajectories starting from different initial conditions but corresponding to the same switching signal and input voltage evolutions will exponentially converge to zero, and that the exponential convergence rate can be uniform over all the switching signals considered. As regards the open-loop inverter operation strategy of Cao et al. (2011) explained in Section 2.4, it follows that if the assumptions on the load are satisfied, then the steady-state trajectory corresponding to the duty cycle evolution (15) will be reached irrespective of the initial condition. If the load is linear but possibly time-varying (i.e. $R(t, x_l) = \bar{R}(t)$ and/or $h(t, v) = \bar{\alpha}(t)v$), then the assumptions of Theorem 2 are satisfied whenever the assumptions on the load given in Section 2.3 are. The inverter connected to a linear time-invariant resistive load corresponds to the prototype tested by Cao et al. (2011).

4. Uncontrolled Conduction Mode (UCM)

The aim of this section is to show that under constraints on the load similar to those required in Section 3, the transience or persistence of UCM, for switching signals in the class considered, is independent of initial conditions. We remark that the occurrence of UCM is not a consequence of intentionally triggering both transistors at the same time, and depends on the value of the state variables. In this regard, UCM in the semi-quasi-Z-source inverter bears some similarity to Mode 5 of the Z-source inverter as reported in Section 2 of Shen and Peng (2008).

When analyzing UCM, we have to distinguish between (a) the *command signal* $s(t)$ that indicates whether Mode I or Mode II is requested (depending on the gate signal for each transistor, $s(t) \in \{I, II\}$), and (b) the true *switching mode* of the circuit $\sigma(t)$, which depends on $s(t)$ and on the state variables ($\sigma(t) \in \{I, II, III\}$, with $\sigma(t) = III$ meaning UCM). According to Fig. 1 and considering ideal antiparallel diodes, if the capacitor C_1 voltage, v_{C_1}, is greater than $-V_{in}$, then the inverter operates in CCM and $\sigma(t) = s(t)$. However,
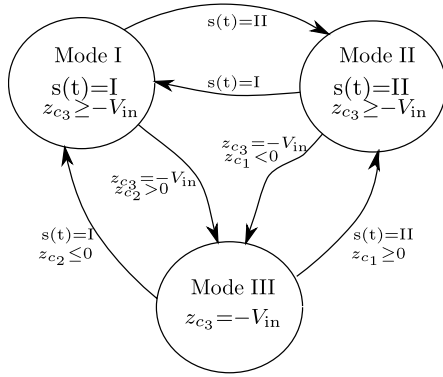
Fig. 4. Switching mode flow diagram for the semi-quasi-Z-source inverter: $z_{c_1} = i_{L_1}$, $z_{c_2} = i_{L_2}$, $z_{c_3} = v_{C_1}$, $z_{c_4} = v_{C_2}$.

if $v_{C_1} = -V_{\text{in}}$, then the inverter may reach Mode III. Fig. 4 shows the true switching mode of the inverter depending on the command signal and state vector z_c as defined in (1). Considering the positive convention for each variable as shown in Fig. 1 and with z_c as in (1), then

$$P_c \dot{z}_c(t) = A_{\sigma(t)}^q z_c(t) + b_{\sigma(t)}^q - e_4 i_o(t), \tag{43}$$

with $\sigma(t) \in \{\text{I, II, III}\}$, A_{I}^q, A_{II}^q, b_{I}^q, b_{II}^q, P_c as in (3)–(5),

$$\text{and} \quad A_{\text{III}}^q = \begin{bmatrix} 0 & 0 & 0 & 0 \\ 0 & 0 & 0 & 1 \\ 0 & 0 & 0 & 0 \\ 0 & -1 & 0 & 0 \end{bmatrix}, \qquad b_{\text{III}}^q = \begin{bmatrix} V_{\text{in}} \\ -V_{\text{in}} \\ 0 \\ 0 \end{bmatrix}. \tag{44}$$

For the sake of clarity, in this section we assume that the input voltage V_{in} is constant, although more general results could be obtained by allowing the input voltage to be time-varying and imposing smoothness assumptions on its time dependence. Direct analysis of either the inverter circuit of Fig. 1 or Eqs. (43) with (3)–(5) and (44) shows that the only state variable whose derivative may be discontinuous at a time instant of continuity of the command signal $s(t)$ is $z_{c_3} = v_{C_1}$, and that the region of the state space given by $z_{c_3} \geq -V_{\text{in}}$ is positively invariant. Capacitor C_1 voltages lower than $-V_{\text{in}}$ would produce impulsive current through C_1 and the instantaneous change to $z_{c_3} = -V_{\text{in}}$, irrespective of which of the two switches S_1 or S_2 is being triggered at that instant. Consequently, the results of this section will be valid for initial conditions satisfying $z_{c_3}(0) \geq -V_{\text{in}}$. Our main results for UCM are given below as Theorem 3.

Theorem 3. *Consider the ideal switched model of the semi-quasi-Z-source inverter that includes UCM, as given by (43), connected to a load of one of the forms (9). Suppose that the load satisfies the assumptions required in Theorem 2. Let ϵ and T satisfy $0 < 2\epsilon \leq T \leq \pi \sqrt{L_1 C_1}$, let $s(t) \in \overline{\mathbb{PWM}}(T, \epsilon)$ and consider an initial condition satisfying $z_{c_3}(0) = v_{C_1}(0) \geq -V_{\text{in}}$. Then*

(a) *The solution exists for all $t \geq 0$, is unique and satisfies $z_{c_3}(t) \geq -V_{\text{in}}$ for all $t \geq 0$.*

(b) *If for the given initial condition and command signal, the voltage across capacitor C_1 satisfies*

$$z_{c_3}(t) = v_{C_1}(t) \geq -V_{\text{in}} + d_3, \tag{45}$$

for all $t \geq 0$ and for some $d_3 > 0$, then, for the same command signal $s(t)$ and each initial condition (satisfying $z_{c_3}(0) \geq -V_{\text{in}}$) there exists a time instant t^* such that $z_{c_3}(t) = v_{C_1}(t) > -V_{\text{in}}$ for all $t > t^*$.◦

For a given command signal $s(t)$, Theorem 3 (b) establishes that if at least one initial condition exists for which the voltage across

capacitor C_1 remains higher than $-V_{\text{in}}$ at all times (and hence the inverter operates in CCM at all times), then every initial condition will have an associated time instant from which the inverter will never leave CCM. This result establishes that the situation where UCM never ceases to occur is independent of the initial condition, and hence only depends on the command signal applied.

5. Conclusions

This work has provided large-signal stability conditions for the ideal switched model of the semi-quasi-Z-source inverter connected to nonlinear time-varying dynamic loads and operating in CCM and UCM. For the inverter operating in CCM, our stability results ensure boundedness of all circuit variables for every switching signal in a specific class. We have also provided conditions under which the difference between two state trajectories that start from different initial conditions and correspond to the same switching signal will decrease exponentially to zero. These results are valid for every possible value of inductances and capacitances of the inverter circuit and can be used to justify the standard open-loop semi-quasi-Z-source inverter operation strategy. We have also established that the transience or persistence of UCM is independent of initial conditions and only depends on the switching command signal. Specifically, if for a given command signal there exists at least one initial condition for which the inverter operates in CCM for all $t \geq 0$, then every initial condition will have an associated time instant from which the inverter will never leave CCM (when operating under the same command signal). These stability results are based on the use of the natural energy function of the circuit as a Lyapunov function. One of the complications in analyzing stability for this inverter is due to the fact that neither of the switching modes of the circuit is asymptotically stable, nor detectable from the output voltage, and hence no Lyapunov function exists whose derivative along the system trajectories has a dominating negative definite term. Stability for the semi-quasi-Z-source inverter is not only dependent on the load but also on the limitations imposed on switching.

Appendix. Proofs

Proof of Lemma 1

The proof is given for a load of the form (9a) or (9b). The proof for loads of the form (9c) is simpler and can be obtained by following the same ideas in this proof. Consider the system $\dot{x}(t) = A(\mu(t))x(t)$. Let μ satisfy

$$\mu(t) = \begin{cases} 0.5 & \text{if } 0 \leq t < t_{\text{I}}, \\ -0.5 & \text{if } t_{\text{I}} \leq t < t_{\text{I}} + t_{\text{II}}, \\ 0.5 & \text{if } t_{\text{I}} + t_{\text{II}} \leq t < t_{\text{I}} + t_{\text{II}} + \epsilon, \end{cases}$$

so that given an initial state $x(0) = x_o$, we have $x(t_{\text{I}} + t_{\text{II}} + \epsilon) = M_\epsilon x_o$. Consider the Lyapunov function $V(x) = x'Px$, so that $\dot{V}(x, \mu) = x'[A(\mu)'P + PA(\mu)]x$. From (21), (23), (25) and (34), we have $A_c'(\mu)P_c + P_c A_c(\mu) = 0$ and $\dot{V}(x, \mu)$ does not depend on μ, so that

$$\dot{V}(x, \mu) =: -x'Nx, \tag{A.1}$$

with N to be determined. From (27) and (10), also

$$\frac{1}{2}(A_I'P_H + P_H A_I) = -P_H \left(\frac{KK'}{4h_m} + \lambda_m I \right) P_H.$$

It thus follows that

$$N = \tilde{N}'\tilde{N} + \begin{bmatrix} 0 & 0 \\ 0 & \lambda_m P_H^2 \end{bmatrix}, \quad \text{and} \tag{A.2}$$

$$\tilde{N} = \begin{cases} \begin{bmatrix} \sqrt{h_m} e_4' & \dfrac{K'P_H}{2\sqrt{h_m}} \end{bmatrix} & \text{if load is PHF,} \\ 0 & \text{if load is PH,} \end{cases} \tag{A.3}$$

and $N \geq 0$. From (A.1), then $\dot{V} \leq 0$. Consequently, for every $\epsilon \geq 0$ then

$$M_\epsilon' P M_\epsilon - P \leq 0, \qquad (M_\epsilon^2)' P M_\epsilon^2 - P \leq 0, \tag{A.4}$$

$$x'(M_\epsilon' P M_\epsilon - P)x < 0 \qquad \Longrightarrow$$

$$x'((M_\epsilon^2)' P M_\epsilon^2 - P)x < 0. \tag{A.5}$$

(a) Let x_o satisfy

$$x_o'(M_\epsilon' P M_\epsilon - P)x_o = 0. \tag{A.6}$$

Let $\mathcal{S}_I$ and $\mathcal{S}_{II}$ denote the largest subspaces invariant under A_I or A_{II}, respectively, and contained in ker N. In order for (A.6) to hold, then the state evolution $x(t)$ that satisfies $x(0) = x_o$ must remain within $\mathcal{S}_I$ for $0 \leq t < t_I$ and $t_I + t_{II} \leq t < t_I + t_{II} + \epsilon$ and within $\mathcal{S}_{II}$ for $t_I \leq t < t_I + t_{II}$. According to (A.2)–(A.3), $x \in \ker N$ implies that

$$x' = \begin{bmatrix} x_c' & 0 \end{bmatrix} \quad \text{and} \quad h_m \begin{bmatrix} x_c' e_4 e_4' x_c \end{bmatrix} = 0, \tag{A.7}$$

with $x_c \in \mathbb{R}^4$. If the load is PHF, then $h_m \neq 0$ and the right-hand equation in (A.7) implies that $e_4' x_c = 0$. The kernel of N can thus be written as $\ker N = \text{span}\{e_1, e_2, e_3\}$, where e_i denotes the ith column of the $n \times n$ identity matrix, with n the system order. The largest subspaces invariant under A_I or A_{II} that are contained in $\ker N$ can be found by the following recursive formula (see, e.g. Wonham, 1985)

$$\nu_1^j = \ker N,$$

$$\nu_{i+1}^j = \nu_i^j \cap \ker(N A_j^{i-1}) \quad \text{with } j \in \{I, II\}, \tag{A.8}$$

yielding $\nu_n^j = \mathcal{S}_j$. We have

$$A_j x = \begin{bmatrix} A_{c_j} + B_c h_m e_4' & B_c[B+K]'P_H \\ B e_4' & A_l \end{bmatrix} \begin{bmatrix} x_c \\ 0 \end{bmatrix} = \begin{bmatrix} A_{c_j} x_c \\ 0 \end{bmatrix},$$

where we have used (A.7) and defined $A_{c_I} := A_c(0.5)$ and $A_{c_{II}} := A_c(-0.5)$. The required invariant subspaces can be straightforwardly computed, yielding

$$\mathcal{S}_I = \text{span}\{e_1\}, \qquad \mathcal{S}_{II} = \text{span}\{e_1, e_3\}. \tag{A.9}$$

In the case of a PH load, $h_m = 0$ and the right-hand equation in (A.7) is trivially satisfied. In this case, we can write $\ker N = \text{Im}[I_4 \ 0]'$, and if $x \in \ker N$, then

$$A_j x = \begin{bmatrix} A_{c_j} & B_c B' P_H \\ B e_4' & A_l \end{bmatrix} \begin{bmatrix} x_c \\ 0 \end{bmatrix} = \begin{bmatrix} A_{c_j} x_c \\ B_l e_4' x_c \end{bmatrix}.$$

Again, the required invariant subspaces can be straightforwardly computed, yielding the same result (A.9). The vector x_o satisfies (A.6) if and only if

$$e^{A_I t} x_o \in \mathcal{S}_I, \quad \text{for all } t \in [0, t_I), \tag{A.10}$$

$$e^{A_{II} t} e^{A_I t_I} x_o \in \mathcal{S}_{II}, \quad \text{for all } t \in [0, t_{II}) \quad \text{and} \tag{A.11}$$

$$e^{A_I t} e^{A_{II} t_{II}} e^{A_I t_I} x_o \in \mathcal{S}_I, \quad \text{for all } t \in [0, \epsilon). \tag{A.12}$$

From (21), (25), (A.10) and (33), it follows that $x_o = e^{A_I t} x_o = \alpha e_1$ for some $\alpha \in \mathbb{R}$ and for all $t \in [0, t_I]$. From (21), (25), (A.11) and (33), then $e^{A_{II} t_{II}} e^{A_I t_I} x_o = \alpha[\cos(\omega t_{II})e_1 + \sqrt{L_1/C_1}\sin(\omega t_{II})e_3]$, with $\omega = 1/\sqrt{L_1 C_1}$. Since $t_{II} < \pi\sqrt{L_1 C_1}$, then $\sin(\omega t_{II}) \neq 0$. Hence, if $\epsilon > 0$, from (A.12) we must have $x_1 := M_0 x_o = e^{A_{II} t_{II}} e^{A_I t_I} x_o \in \mathcal{S}_I$, which implies that $x_o = 0$. Therefore, if $\epsilon > 0$, (A.6) implies that $x_o = 0$ and (36) is established. For $\epsilon = 0$, suppose that $x_o \neq 0$ satisfies (A.6). By the previous argument, $x_1 = M_0 x_o \notin \mathcal{S}_I$ and

$$x_1'(M_0 P M_0 - P)x_1 = x_o'((M_0^2)' P M_0^2 - M_0 P M_0)x_o$$
$$= x_o'((M_0^2)' P M_0^2 - P)x_o < 0,$$

where the latter inequality follows because, repeating the previous argument, $x_1'(M_0' P M_0 - P)x_1 = 0$ would imply that $x_1 \in \mathcal{S}_I$, a contradiction. Recalling (A.4)–(A.5), we conclude that $\rho(M_0^2) < 1$ and hence $\rho(M_0) < 1$.

(b) By (A.4), then $\rho(M_\epsilon) \leq 1$ for all $\epsilon \geq 0$. Take $x_o = e_1$. Then, $e^{A_I t_I} x_o = x_o$ and $e^{A_{II} t_{II}} x_o = \cos(\omega t_{II})e_1 + \sqrt{L_1/C_1}\sin(\omega t_{II})e_3 = (-1)^k e_1 = (-1)^k x_o$. Therefore, $M_\epsilon x_o = (-1)^k x_o$, showing that $\lambda = (-1)^k$ is an eigenvalue of M_ϵ with $|\lambda| = 1$. $\square$

Proof of Theorem 1

Local existence of solutions from every (finite) initial condition is ensured by the fact that, according to the assumptions, the right-hand side of (32) is piecewise continuous in t for all x, continuous in x for all t, and bounded in t for every fixed x (see, e.g., Theorem 1, §1 of Filippov (1988)).

Next, we show that if a solution has a finite time of existence, then it must be bounded for as long as it exists. From (11) and (30), we have $\forall v$,

$$0 \leq v\rho(t, v) \leq (h_M - h_m)v^2, \quad \text{hence} \tag{A.13}$$

$$\rho^2(t, v) \leq (h_M - h_m)^2 v^2. \tag{A.14}$$

Let $V(x) = x'Px$, with P as in (34). Then

$$\kappa_1 \|x\|^2 \leq V(x) \leq \kappa_2 \|x\|^2, \quad \forall x \tag{A.15}$$

with $\kappa_1 > 0$ because P is positive definite. The derivative of $V(x)$ along the trajectories of (32) satisfies

$$\dot{V} = x'\left(A(\mu)'P + PA(\mu)\right)x + 2x'PF + 2uB_s'Px$$
$$= -x'Nx + 2x'PF + 2uB_s'Px$$
$$\leq -x'Nx + x_c'P_c B_{in}u, \tag{A.16}$$

with $N \geq 0$ as in (A.2)–(A.3), where we have used (26) and (34), and the inequality above follows because $2x'PF \leq 0$. This latter point, follows from (34), (22), (28), (29), (A.13) and (12). Define

$$\|u_{[a,b]}\| := \sup_{\tau \in [a,b]} \|u(\tau)\|. \tag{A.17}$$

From (A.16), taking (A.2)–(A.3) into account, it follows that for $t \geq 0$ we have

$$\dot{V}(x) \leq \frac{\|PB\| \, \|u_{[0,t]}\|}{\sqrt{\kappa_1}} \sqrt{V(x)}, \tag{A.18}$$

where we have used (A.15). Applying the comparison lemma for $t \geq 0$ (see, e.g. Khalil, 2002) to (A.18), yields

$$\sqrt{V(x(t))} \leq \sqrt{V(x(0))} + \frac{\|PB_{in}\|}{\sqrt{\kappa_1}} \int_0^t \|u_{[0,\tau]}\| d\tau. \tag{A.19}$$

From this inequality, it follows that $V(x(t))$ cannot become unbounded in finite time, and hence neither can $x(t)$. We have thus shown that if a solution has a finite time of existence, then it is bounded for as long as it exists. Next, suppose that a solution $x(t)$ exists for $t \in [0, t_{max})$. Since $x(t)$ is absolutely continuous and bounded for all $t \in [0, t_{max})$, then the left limit $x^- := \lim_{t \to t_{max}^-} x(t)$ exists and is a finite value. Next, considering the initial condition $x(t_{max}) = x^-$, we can extend the solution beyond t_{max} by applying our local existence result above. Then, every Carathéodory solution is ensured to exist for all $t \geq 0$.

We proceed to establish (37). Write (32) as follows:

$$\dot{x}(t) = A(\mu(t))x(t) + w(t) \tag{A.20}$$

$$w(t) := F(t, x(t)) + B_s u(t). \tag{A.21}$$

Since $\mu(t) \in \overline{\mathbb{PWM}}(T, \epsilon)$, we have

$$\mu(t) = \begin{cases} 0.5 & \text{if } r_k \leq t < r_k + t_{I,k}, \\ -0.5 & \text{if } r_k + t_{I,k} \leq t < r_{k+1} \end{cases} \tag{A.22}$$

for constants $t_{I,k}$ such that $\epsilon \leq t_{I,k} \leq r_{k+1} - r_k - \epsilon$. Let $t_{II,k} = r_{k+1} - r_k - t_{I,k}$ so that also $\epsilon \leq t_{II,k} \leq r_{k+1} - r_k - \epsilon$. Consider time instants of the form $t_k = r_k + \epsilon/2$. Let $\tilde{\Phi}(t, s)$ be the state transition matrix of the linear system (A.20), so that $\tilde{\Phi}(s, s) = I$ for all s. Define $\Phi(t, t_k) := \tilde{\Phi}(t + t_k, t_k)$. From (A.20) and (A.22), we have

$$\Phi(t, t_k) = \begin{cases} e^{A_I t} & \text{if } 0 \leq t < \tilde{t}_{I,k}, \\ e^{A_{II}(t - \tilde{t}_{I,k})} e^{A_I \tilde{t}_{I,k}} & \text{if } \tilde{t}_{I,k} \leq t < T_k - \dfrac{\epsilon}{2}, \\ e^{A_I(t - T_k + \epsilon/2)} e^{A_{II} t_{II,k}} e^{A_I \tilde{t}_{I,k}} & \text{if } T_k - \dfrac{\epsilon}{2} \leq t \leq T_k, \end{cases}$$

with $\tilde{t}_{I,k} = t_{I,k} - \epsilon/2$ and $T_k = r_{k+1} - r_k$. Define

$$\Phi_k := \Phi(T_k, t_k) = \tilde{\Phi}(t_{k+1}, t_k), \tag{A.23}$$

$$\Xi(\tilde{t}_I, t_{II}) := e^{A_I \epsilon/2} e^{A_{II} t_{II}} e^{A_I \tilde{t}_I}. \tag{A.24}$$

Note that $\Phi_k = \Xi(\tilde{t}_{I,k}, t_{II,k})$. From (A.20)

$$x(t_{k+1}) = \Phi_k x(t_k) + \int_{t_k}^{t_{k+1}} \Phi(t_{k+1} - \tau, t_k) w(\tau) d\tau.$$

Multiplying the above equation on the left by $P^{\frac{1}{2}}$ and evaluating the squared norm yields

$$V(x(t_{k+1})) \leq (1 + \beta) x'(t_k) \Phi_k' P \Phi_k x(t_k) + \left(1 + \frac{1}{\beta}\right) \left\| P^{\frac{1}{2}} \int_{t_k}^{t_{k+1}} \Phi(t_{k+1} - \tau, t_k) w(\tau) d\tau \right\|^2, \tag{A.25}$$

with $\beta \in (0, \infty)$ to be determined. Define

$$R(\tilde{t}_I, t_{II}) := \Xi(\tilde{t}_I, t_{II})' P \Xi(\tilde{t}_I, t_{II}) - P, \tag{A.26}$$

$$\kappa_3 := \inf_{\substack{t_{II} \in [\epsilon, T - \epsilon] \\ \tilde{t}_I \in \left[\frac{\epsilon}{2}, T - t_{II} - \epsilon/2\right]}} \lambda_{\min}[-R(\tilde{t}_I, t_{II})], \tag{A.27}$$

where $\lambda_{\min}$ denotes the least eigenvalue. From Lemma 1(a), it follows that $R(\tilde{t}_I, t_{II}) < 0$ for all $\tilde{t}_I > 0$ and $0 < t_{II} < \pi \sqrt{L_1 C_1}$. Since $\Xi(\cdot, \cdot)$ is continuous on its arguments, the infimum in (A.27) is taken over a compact set, and $0 < 2\epsilon \leq T \leq \pi \sqrt{L_1 C_1}$, then $\kappa_3 > 0$. Since $\Phi_k = \Xi(\tilde{t}_{I,k}, t_{II,k})$, it follows that

$$x' \left(\Phi_k' P \Phi_k - P\right) x \leq -\kappa_3 \|x\|^2, \quad \forall k. \tag{A.28}$$

Combining (A.15) and (A.28), it follows that

$$\Phi_k' P \Phi_k \leq \varrho^2 P \tag{A.29}$$

with $0 < \varrho = \sqrt{1 - \frac{\kappa_3}{\kappa_2}} < 1$. Define $V_k := V(x(t_k))$, select $\beta = \frac{1 - \varrho}{\varrho} > 0$ and employ (A.25) and (A.29)

$$V_{k+1} \leq \varrho V_k + \frac{1}{1 - \varrho} \left\| P^{\frac{1}{2}} \int_{t_k}^{t_{k+1}} \Phi(t_{k+1} - \tau, t_k) w(\tau) d\tau \right\|^2.$$

Define $\bar{\Phi} := \sup_{\substack{t \in [0, \tilde{t}_I + t_{II} + \frac{\epsilon}{2}] \\ t_{II} \in [\epsilon, T - \epsilon] \\ \tilde{t}_I \in [\frac{\epsilon}{2}, T - t_{II} - \epsilon/2]}} \|\Phi(t, t_k)\|$. Combining with (A.21), we can write

$$V_{k+1} \leq \varrho V_k + \Psi_{k,1} + \Psi_{k,2}, \tag{A.30}$$

$$\Psi_{k,2} \leq \frac{2\|P\| \bar{\Phi}^2}{1 - \varrho} \|B_s\|^2 \|u_{[t_k, t_{k+1}]}\|^2 T^2, \tag{A.31}$$

$$\Psi_{k,1} \leq \frac{2\|P\| \bar{\Phi}^2}{(1 - \varrho)} \left| \int_{t_k}^{t_{k+1}} \|F(\tau, x(\tau))\| d\tau \right|^2. \tag{A.32}$$

Using the Schwarz inequality in (A.32) yields

$$\Psi_{k,1} \leq \frac{2\|P\| \bar{\Phi}^2}{(1 - \varrho)} T \int_{t_k}^{t_{k+1}} \|F(\tau, x(\tau))\|^2 d\tau. \tag{A.33}$$

We next proceed for a PHF load, and later particularize to the other load types. From (28), (5) and (22), then

$$\|F(t, x)\|^2 = \frac{1}{C_2^2} \rho^2(t, e_4' x_c) + \|\delta(t, x_l) P_H x_l\|^2, \tag{A.34}$$

and from (12) and (29) it follows that

$$x_l' P_H \delta^2(x_l) P_H x_l \leq (\lambda_M - \lambda_m)^2 \|P_H x_l\|^2. \tag{A.35}$$

Considering (A.34), (A.14) and (A.35), we have

$$\|F(t, x)\|^2 \leq \gamma \left(\|e_4' x_c\|^2 + \|P_H x_l\|^2\right), \tag{A.36}$$

where $\gamma = \max \left\{(h_M - h_m)^2 / C_2^2; (\lambda_M - \lambda_m)^2\right\}$. Using (A.36) in (A.33), then

$$\Psi_{k,1} \leq \frac{2\|P\| \bar{\Phi}^2 T \gamma}{(1 - \varrho)} \int_{t_k}^{t_{k+1}} \left(\|e_4' x_c\|^2 + \|P_H x_l\|^2\right) d\tau. \tag{A.37}$$

From (A.2)–(A.3), it follows that

$$x' N x = \begin{bmatrix} e_4' x_c \\ P_H x_l \end{bmatrix}' \begin{bmatrix} h_m & K'/2 \\ K/2 & \dfrac{KK'}{4 h_m} + \lambda_m I \end{bmatrix} \begin{bmatrix} e_4' x_c \\ P_H x_l \end{bmatrix}$$

$$\geq \alpha_m \left(\|e_4' x_c\|^2 + \|P_H x_l\|^2\right). \tag{A.38}$$

Combining (A.16) and (A.38), it follows that

$$\|e_4' x_c\|^2 + \|P_H x_l\|^2 \leq (-\dot{V} + x_c' P_c B_{in} u) / \alpha_m. \tag{A.39}$$

Combining (A.37) and (A.39), and integrating the term involving $\dot{V}$, we can write

$$\Psi_{k,1} \leq c_1(V_k - V_{k+1}) + c_2 \|u_{[t_k, t_{k+1}]}\| \int_{t_k}^{t_{k+1}} \|x(\tau)\| d\tau, \tag{A.40}$$

for some positive constants c_1 and c_2. We next will bound the integral on the right-hand side of (A.40). According to (A.19) we can write

$$\sqrt{V(x(t))} \leq \sqrt{V_k} + \frac{\|P B_{in}\|}{\sqrt{\kappa_1}} \int_{t_k}^{t} \|u_{[t_k, \tau]}\| d\tau, \tag{A.41}$$

for $t_k \leq t \leq t_{k+1}$. Note from (A.15) that $\|x\| \leq \sqrt{V(x)/\kappa_1}$, combine the latter with (A.40), and employ the above bound on $\sqrt{V(x(t))}$ to arrive at

$$\Psi_{k,1} \leq c_1(V_k - V_{k+1}) + c_3 \|u_{[t_k, t_{k+1}]}\| \sqrt{V_k} + c_5 \|u_{[t_k, t_{k+1}]}\|^2, \tag{A.42}$$

where $c_3 = \frac{c_2}{\sqrt{\kappa_1}} T$, $c_4 = \frac{c_2}{\kappa_1} \|P B_{in}\|$ and $c_5 = c_4 \frac{T^2}{2}$. Combining (A.30), (A.31) and (A.42), we can write

$$V_{k+1} \leq \frac{\varrho + c_1}{1 + c_1} V_k + c_6 \|u_{[t_k, t_{k+1}]}\| \sqrt{V_k} + c_7 \|u_{[t_k, t_{k+1}]}\|^2,$$

with $c_6 = \frac{c_3}{1 + c_1}$, $c_7 = \frac{\|P\| \bar{\Phi}^2 \|B_s\|^2 T^2 2}{(1 - \varrho)(1 + c_1)} + \frac{c_5}{(1 + c_1)}$, and where $0 < \frac{\varrho + c_1}{1 + c_1} < 1$. From this point on, the proof proceeds along standard lines in Lyapunov- and ISS-related derivations (Khalil, 2002), and employs (A.15) and (A.18) in order to reach (37).

If the load is PH, i.e. of the form (9b), then the bound on $\|F(t, x)\|$ in (A.34) holds with $\rho \equiv 0$, (A.36) is replaced by $\|F(t, x)\|^2 \leq (\lambda_M - \lambda_m)^2 \|P_H x_l\|^2$, (A.38) is replaced by $-x' N x \leq -\lambda_m \|P_H x_l\|^2$, and (A.39) by $\|P_H x_l\|^2 \leq (-\dot{V} + x_c' P_c B_{in} u)/\lambda_m$. The rest of the proof for a PH load follows similarly to the PHF load case. If the load is TVS, i.e. of the form (9c), then (A.34) holds with $\delta \equiv 0$,

(A.36) is replaced by $\|F(t,x)\|^2 \le \frac{(h_M - h_m)^2}{C_2^2}\|e_4' x_c\|^2$, and (A.39) by

$\|e_4' x_c\|^2 \le (-\dot{V} + x_c' P_c B_{\text{in}} u)/h_m$. The rest of the proof for a TVS load follows similarly to the PHF load case.

Finally, suppose that the continuous functions $R(t,x_l)$ and/or $h(t,x_l)$, depending on the load type, are such that $F(t,x)$ in (28)–(30) is locally Lipschitz in x for all $t \ge 0$. In this case, the right-hand side of (A.20) is locally Lipschitz in x for all $t \ge 0$. The right-hand side of (A.20) is piecewise continuous in t and every solution of (A.20) satisfies (37). Then, uniqueness of the solutions follows from, e.g., Theorem 3.3 of Khalil (2002). □

Proof of Theorem 2

(a) First, we highlight that taking into account the assumptions on the signal $u(t)$ and the fact that $\mu(t) \in \overline{\text{PWM}}(T, \epsilon)$, the right-hand side of (32) is piecewise continuous in t. Second, we prove that under the assumptions on the load the right-hand side of (32) is globally Lipschitz in x, uniformly in $t \ge 0$. To see this, define

$$f(t,x) := A(\mu(t))x + F(t,x) + B_s u(t), \tag{A.43}$$
$$\xi(t) := x(t) - y(t), \tag{A.44}$$

with x partitioned according to the converter and load dimensions, $x' = [x_c'\ x_l']$ and hence $\xi' = [\xi_c'\ \xi_l'] = [(x_c - y_c)'\ (x_l - y_l)']$. Then

$$\|f(t,x) - f(t,y)\| \le \bar{A}\|x - y\| + \|F(t,x) - F(t,y)\|, \tag{A.45}$$

with $\bar{A} = \max\{\|A(0.5)\|, \|A(-0.5)\|\}$. We have,

$$\|F(t,x) - F(t,y)\| = \left\| \begin{matrix} B_c\left(\rho(t, e_4' x_c) - \rho(t, e_4' y_c)\right) \\ \delta(t, y_l)P_H y_l - \delta(t, x_l)P_H x_l \end{matrix} \right\|.$$

Operating on (38) and (30) it follows that

$$|\rho(t, e_4' x_c) - \rho(t, e_4' y_c)| \le (h_M - h_m)|e_4'(x_c - y_c)|,$$

then $\|B_c\left(\rho(t, e_4' x_c) - \rho(t, e_4' y_c)\right)\| \le \alpha_h \|x - y\|$, (A.46)

where $\alpha_h = (h_M - h_m)\|B_c\|$. In addition, we have

$$\delta(t, y_l)P_H y_l - \delta(t, x_l)P_H x_l = -\tilde{\delta}(t, y_l, \xi_l)$$
$$= [R(t, y_l) - R(t, \xi_l + y_l)]P_H y_l$$
$$- \left(R(t, \xi_l + y_l) - \frac{KK'}{4h_m} - \lambda_m I\right)P_H \xi_l.$$

Considering (41) and (39) then

$$\|\tilde{\delta}(t, y_l, \xi_l)\| \le \sqrt{a}\|P_H \xi_l\| \le \bar{a}\|x - y\|, \tag{A.47}$$

with $\bar{a} = \|P_H\|\sqrt{a}$. From (A.45) and the bounds derived above, it follows that $f(t,x)$ is globally Lipschitz in x, uniformly in $t \ge 0$. Global Lipschitzity of $f(t,x)$ for the case of loads of the form PH and TVS follows analogously. According to, e.g., Theorem 3.2 of Khalil (2002), the state equation $\dot{x}(t) = f(t,x)$, with $x(0) = x_0$, has a unique solution $\forall t \ge 0$.

(b) As in the proof of Theorem 1 we proceed for a PHF load and then particularize to the other load types. Let $\varepsilon(t) = x^{\mu,u}(t, x_{10}) - x^{\mu,u}(t, x_{20})$. From (32) we have

$$\dot{\varepsilon} = A(\mu)\varepsilon - \Sigma(t, x, \varepsilon), \quad \text{where} \tag{A.48}$$

$$\Sigma'(t, x, \varepsilon) = \left[\frac{e_4'}{C_2}\tilde{\rho}(t, x_{2c_4}, \varepsilon_{c_4})\quad \tilde{\delta}'(t, x_{2l}, \varepsilon_l)\right], \tag{A.49}$$

with $x_{2c_4}(t) = e_4' x_{2c}$, $x^{\mu,u}(t, x_{20}) = [x_{2c}'\ x_{2l}']'$, $\varepsilon' = [\varepsilon_c'\ \varepsilon_l']$ and $\varepsilon_{c_4}(t) = e_4' \varepsilon_c$, and where

$$\tilde{\rho}(t, x_{2c_4}, \varepsilon_{c_4}) := \rho(t, x_{2c_4} + \varepsilon_{c_4}) - \rho(t, x_{2c_4}) \tag{A.50}$$

$$\tilde{\delta}(t, x_{2l}, \varepsilon_l) = \delta(t, x_{2l} + \varepsilon_l)P_H(x_{2l} + \varepsilon_l)$$
$$- \delta(t, x_{2l})P_H x_{2l}. \tag{A.51}$$

From (30) and (38), it follows that for all t, x_{2c_4},

$$0 \le \varepsilon_{c_4}\tilde{\rho}(t, x_{2c_4}, \varepsilon_{c_4}) \le (h_M - h_m)\varepsilon_{c_4}^2 \text{ hence} \tag{A.52}$$
$$0 \le \tilde{\rho}^2(t, x_{2c_4}, \varepsilon_{c_4}) \le \varepsilon_{c_4}^2 (h_M - h_m)^2. \tag{A.53}$$

Consider time instants $t_k = r_k + \epsilon/2$ with r_k according to Definition 1, and write

$$\varepsilon(t_{k+1}) = \Phi_k \varepsilon(t_k) - \int_{t_k}^{t_{k+1}} \Phi(t_{k+1} - \tau, t_k)\Sigma(\tau, x, \varepsilon)d\tau,$$

with Φ_k and $\Phi(\cdot, \cdot)$ as in the proof of Theorem 1. Consider the Lyapunov function $V(\varepsilon) = \varepsilon'P\varepsilon$ with P from (34), and define $V_k := V(\varepsilon(t_k))$. Following similar lines as in the proof of Theorem 1, we can write

$$V_{k+1} \le \varrho V_k + \frac{2T\|P\|\bar{\Phi}}{(1-\varrho)}\int_{t_k}^{t_{k+1}} \|\Sigma(\tau, x, \varepsilon)\|^2 d\tau, \tag{A.54}$$

with $0 < \varrho < 1$. Note that

$$\|\Sigma(t, x, \varepsilon)\|^2 = \frac{\left\|\tilde{\rho}(t, x_{2c_4}, \varepsilon_{c_4})\right\|^2}{C_2^2} + \left\|\tilde{\delta}(t, x_{2l}, \varepsilon_l)\right\|^2, \tag{A.55}$$

and from (39) we have $\left\|\tilde{\delta}(t, x_{2l}, \varepsilon_l)\right\|^2 \le a\|P_H \varepsilon_l\|^2$. Using the latter inequality and (A.53), we can write

$$\|\Sigma(t, x, \varepsilon)\|^2 \le \gamma\left(\varepsilon_{c_4}^2 + \|P_H \varepsilon_l\|^2\right), \tag{A.56}$$

where $\gamma = \max\left\{(h_M - h_m)^2/C_2^2;\ a\right\}$. Considering (A.56) in (A.54), it follows that

$$V_{k+1} \le \varrho V_k + \frac{2T\|P\|\bar{\Phi}^2}{1-\varrho}\gamma\int_{t_k}^{t_{k+1}}\left(\varepsilon_{c_4}^2 + \|P_H \varepsilon_l\|^2\right)d\tau. \tag{A.57}$$

The time derivative of $V(\varepsilon) = \varepsilon'P\varepsilon$ along the trajectories of (A.48) satisfies

$$\dot{V}(\varepsilon) = -\varepsilon'N\varepsilon - \varepsilon_{c_4}\tilde{\rho}(t, x_{2c_4}, \varepsilon_{c_4}) - \tilde{\delta}'(t, x_{2l}, \varepsilon_l)P_H \varepsilon_l, \tag{A.58}$$

where the matrix N is as in (A.2)–(A.3). From (A.38), (A.52) and (40) it follows that

$$\|\varepsilon_{c_4}\|^2 + \|P_H \varepsilon_l\|^2 \le -\dot{V}(\varepsilon)/\alpha_m. \tag{A.59}$$

Considering (A.59) in (A.57) we have

$$V_{k+1} \le \varrho V_k + c_1 \int_{t_k}^{t_{k+1}} -\dot{V}(\varepsilon(\tau))d\tau,$$

where $c_1 = \frac{2T\|P\|\bar{\Phi}^2}{1-\varrho}\frac{\gamma}{\alpha_m}$. Solving the integral above, we arrive at $V_{k+1} \le \frac{\varrho+c_1}{1+c_1}V_k$, where $0 < \frac{\varrho+c_1}{1+c_1} < 1$. It follows that $V_k \le \left(\frac{\varrho+c_1}{1+c_1}\right)^k V_0$. Noting that $\dot{V}(\varepsilon) \le 0$, and recalling that $t_0 = \epsilon/2$, we obtain the following bound

$$V(\varepsilon(t)) \le e^{r(\frac{\epsilon}{2}+T)}e^{-rt}V(\varepsilon(0)), \quad \forall t \ge 0,$$

$$r := -\log\left(\frac{\varrho+c_1}{1+c_1}\right)\frac{1}{T} > 0,$$

whence the required bound for $\|\varepsilon(t)\|$ follows by (A.15).

If the load is PH, then the bound on $\|\Sigma(t, x, \varepsilon)\|$ in (A.55) holds with $\tilde{\rho} \equiv 0$, (A.56) is replaced by $\|\Sigma(t, x, \varepsilon)\|^2 \le a\|P_H \varepsilon_l\|^2$, (A.58) is replaced by $\dot{V}(\varepsilon) = -\lambda_m \|P_H \varepsilon_l\|^2 - \tilde{\delta}(t, x_{1l}, \varepsilon_l)P_H \varepsilon_l$ and (A.59) by $\|P_H \varepsilon_l\|^2 \le -\dot{V}(\varepsilon)/\lambda_m$. The rest of the proof for a PH load follows similarly to the PHF load case. If the load is TVS, then (A.55) holds with $\tilde{\delta} \equiv 0$, (A.56) is replaced by $\|\Sigma(t, x, \varepsilon)\|^2 \le \frac{(h_M - h_m)^2}{C_2^2}\|e_4' \varepsilon_c\|^2$,

(A.58) is replaced by $\dot{V}(\varepsilon) = -h_m \|\varepsilon_{c_4}\|^2 - \varepsilon_{c_4}\tilde{\rho}(t, x_{2c_4}, \varepsilon_{c_4})$ and (A.59) by $\varepsilon_{c_4}^2 \le -\dot{V}(\varepsilon)/h_m$. The rest of the proof for a TVS load follows similarly to the PHF load case. □

Proof of Theorem 3

(a) Consider the following auxiliary equations:

$$P_c \dot{z}_c(t) = A^q_{\{s(t),z_{c_3}(t)\}} z_c(t) + b^q_{s(t)} - e_4 i_o(t),$$

$$A^q_{\{s(t),z_{c_3}(t)\}} = \begin{cases} A^q_{s(t)} & \text{if } z_{c_3}(t) > -V_{\text{in}}, \\ \begin{bmatrix} 1 & 0 & 0 & 0 \\ 0 & 1 & 0 & 0 \\ 0 & 0 & b(t) & 0 \\ 0 & 0 & 0 & 1 \end{bmatrix} A^q_{s(t)} & \text{if } z_{c_3}(t) < -V_{\text{in}}, \end{cases}$$

also with $v_o = e'_4 z_c$, and where the time-dependent coefficient $b(t)$ is such that

$$C_1 \dot{z}_{c_3} = \begin{cases} |z_{c_2}| & \text{if } s(t) = \text{I}, \\ |z_{c_1}| & \text{if } s(t) = \text{II}. \end{cases} \tag{A.60}$$

Consider the system represented by the interconnection of the auxiliary system above with the corresponding load equations, depending on the load type. Let $z := [z'_c \; x'_l]'$ denote the state of this auxiliary system (with $z = z_c$ if the load is TVS). We have

$$\dot{z} = f(t, z), \tag{A.61}$$

where f is piecewise continuous in t (dependence on $s(t)$), and continuous in z for every t whenever $z_{c_3} \neq -V_{\text{in}}$. Solutions to (A.61) in the sense of Filippov are solutions to the differential inclusion $\dot{z} \in \mathcal{F}(t, z)$,

$$\mathcal{F}(t, z) = \begin{cases} \{f(t, z)\} & \text{if } z_{c_3} \neq -V_{\text{in}}, \\ \text{conv}\{f^-(t, z), f^+(t, z)\} & \text{if } z_{c_3} = -V_{\text{in}}, \end{cases}$$

where $f^-(t, z)$ and $f^+(t, z)$ are the limits of $f(t, z)$ when z is approached from the region $z_{c_3} < -V_{\text{in}}$ and $z_{c_3} > -V_{\text{in}}$, respectively. The set-valued function $\mathcal{F}$ is upper semi-continuous in (t, x) during each interval of continuity of the right-continuous command signal $s(t)$, with nonempty, convex and compact values, and hence at least one (forward) solution exists for every initial condition, at least during a sufficiently small time interval (see, e.g., Theorem 1, §7 of Filippov, 1988).

It is easy to see that the only component of $\dot{z}(t)$ which may be discontinuous at a time instant of continuity of the command signal $s(t)$ is $\dot{z}_{c_3}(t)$, and that this discontinuity occurs when $z_{c_3}(t)$ reaches the value $-V_{\text{in}}$. Note that if the state trajectory hits the discontinuity surface given by $z_{c_3} = -V_{\text{in}}$ either when (i) $z_{c_2}(t) > 0$ and $s(t) = \text{I}$ or (ii) when $z_{c_1}(t) < 0$ and $s(t) = \text{II}$, then the trajectory cannot leave the surface until (i) or (ii) ceases to hold, since on both sides trajectories point towards the surface [recall (A.60)]. Therefore, the only possible solution if condition (i) or (ii) is true is one such that $\dot{z}_{c_3} = 0$. The trajectory can leave the surface only when $z_{c_2}(t) \leq 0$ if $s(t) = \text{I}$ or when $z_{c_1}(t) \geq 0$ if $s(t) = \text{II}$. This analysis of the behavior of trajectories of the differential inclusion above when $z_{c_3}(t) = -V_{\text{in}}$ shows that z satisfies (A.61) in the sense of Filippov if and only if z satisfies (43) jointly with the load equations, according to the flow diagram of Fig. 4. Then, in the region given by $z_{c_3} \geq -V_{\text{in}}$ a solution in the sense of Filippov for system (A.61) is equivalent to a solution in the sense of Carathéodory for system (43).

We next show that the region $z_{c_3} \geq -V_{\text{in}}$ is positively invariant. Consider an initial condition $z(0)$ satisfying $z_{c_3}(0) = -V_{\text{in}}$. For a contradiction, suppose that for some t_1 sufficiently small so that the solution still exists, it happens that $z_{c_3}(t_1) < -V_{\text{in}}$. Then, there must exist $0 < t_3 < t_2 < t_1$ so that $z_{c_3}(t) < -V_{\text{in}}$ and $\dot{z}_{c_3}(t) < 0$ for almost all $t_3 < t < t_2$. Since z_{c_3} is absolutely continuous, the latter fact contradicts (A.60). We have thus shown that if $z(0)$ satisfies $z_{c_3}(0) \geq -V_{\text{in}}$, then $z_{c_3}(t) \geq -V_{\text{in}}$ for all $t \geq 0$ for which the solution exists.

We next establish uniqueness of solutions (right-uniqueness in Filippov, 1988). Recall that under the assumptions of Theorem 2,

we have that $f(t, z)$ in (A.61) is Lipschitz in z, uniformly in t in the region $z_{c_3} > -V_{\text{in}}$. The same can be shown for the auxiliary system in the region $z_{c_3} < -V_{\text{in}}$. According to the auxiliary system equations, we have

$$\bar{h}(t, z) := f^+(t, z) - f^-(t, z) = c_{s(t)}(z) e_3,$$

$$c_{s(t)}(z) = \begin{cases} 0 & \text{if } s(t) = \text{I} \quad \text{and } z_{c_2} \leq 0, \\ 0 & \text{if } s(t) = \text{II} \quad \text{and } z_{c_1} \geq 0, \\ -2z_{c_2} & \text{if } s(t) = \text{I} \quad \text{and } z_{c_2} > 0, \\ 2z_{c_1} & \text{if } s(t) = \text{II} \quad \text{and } z_{c_1} < 0. \end{cases}$$

Note that the discontinuity vector $\bar{h}(t, z)$ is directed along the normal to the discontinuity surface $z_{c_3} = -V_{\text{in}}$, and that $e'_3 \bar{h}(t, z) = c_{s(t)}(z) \leq 0$ for all (t, z). According to Lemma 3, §10 of Filippov (1988), then every solution is right-unique in a neighborhood of every point of the discontinuity surface.

Therefore we have established existence and uniqueness of the solution in the sense of Filippov of system (A.61) at least for a sufficiently small time. Next, we show that every solution is bounded for as long as it exists. Consider as Lyapunov function the natural energy function of the inverter, given by $V(z) = z'Pz$ with P as in (34). Since the load connected to the inverter is strictly passive and only the input voltage source can deliver energy to the circuit, then the derivative of the Lyapunov function along the trajectories of system (43) satisfies

$$\dot{V}(z) \leq V_{\text{in}} \left(|z_{c_1}| + |z_{c_2}| \right) \leq V_{\text{in}} \|z\| \sqrt{n} \leq V_{\text{in}} \frac{\sqrt{n}}{\sqrt{k_1}} \sqrt{V(z)},$$

where n is the dimension of z and we have used (A.15). Applying the comparison lemma (see, e.g. Khalil, 2002) yields

$$\sqrt{V(z)} \leq \sqrt{V(z(0))} + V_{\text{in}} \sqrt{n}/(2\sqrt{k_1}) t \tag{A.62}$$

for $t \geq 0$. From (A.62), it follows that the energy function, and hence the trajectory z, cannot become unbounded in finite time. Therefore, if the solution has a finite time of existence, then it is bounded. The latter fact, jointly with the absolute continuity of z while it exists and the local existence previously established, can be used to show that the solution must exist for all $t \geq 0$.

(b) Consider $z_1(t) := z^s(t, y_o)$ and $z_2(t) := z^s(t, x_o)$, where z^s denotes the solution to (43) with the inverter connected to a load of one of the forms in Section 2.3, corresponding to initial conditions y_o and x_o, respectively, and command signal $s(t)$. Let x_o denote the given initial condition, for which (45) holds. The vectors z_1 and z_2 are partitioned as $z'_1 = [z'_{1c} z'_{1l}]$ and $z'_2 = [z'_{2c} z'_{2l}]$, where $z_{1c}, z_{2c} \in \mathbb{R}^4$ correspond to the state vector (1), and z_{1l}, z_{2l} correspond to the load state vector x_l in (9). Let $\varepsilon(t) := z_1(t) - z_2(t)$. Considering the switched system (43), the loads given by (9), and the variable ε, we can write

$$\dot{\varepsilon}(t) = A(s)\varepsilon(t) + B_d \tilde{u}(t) - \Sigma(t, z, \varepsilon), \tag{A.63}$$

$$\tilde{u}(t) := \left[P_{\text{I}}(t) z_{1c_2}(t) - P_{\text{II}}(t) z_{1c_1}(t) \right], \tag{A.64}$$

$$P_i(t) = \begin{cases} 1 & \text{if } s(t) = i \text{ and } \sigma(t) = \text{III}, \\ 0 & \text{otherwise}, \end{cases} \tag{A.65}$$

with $i \in \{\text{I}, \text{II}\}$ and where $\sigma(t)$ is the true switching mode of the solution $z_1(t)$. By assumption, the solution $z_2(t)$ never enters UCM (i.e. Mode III), and if the same happens for $z_1(t)$, then $\tilde{u}(t) \equiv 0$ and (A.63) becomes equivalent to (A.48). The rest of the quantities involved in (A.63) depend on the load type, as follows

- If the load is PHF, then $A(s)$ is as in (25), Σ is as in (A.49),

$$\varepsilon := \begin{bmatrix} \varepsilon_c \\ \varepsilon_l \end{bmatrix}, \qquad B_d = \begin{bmatrix} \bar{B}_d \\ 0 \end{bmatrix} \quad \text{with } \bar{B}_d = [0 \quad 0 \quad \frac{1}{C_1} \quad 0]'. \tag{A.66}$$

- If the load is PH, then $A(s)$ is as in (25) with $h_m = 0$ and $K = 0$, and (A.49) and (A.66) hold with $\tilde{\rho} := 0$.

- If the load is TVS, then $A(s)$ is as in (31),

$$\varepsilon := \varepsilon_c, \qquad B_d = \bar{B}_d, \qquad \Sigma(t, z, \varepsilon) = B_c \tilde{\rho}(t, z_{2c_4}, \varepsilon_{c_4}).$$

The variables $\tilde{\rho}$ and $\tilde{\delta}$ are as in (A.50)–(A.51). Note that the command signal $s(t)$ corresponds to the switching signal $\mu(t)$ in (25) and (31) as follows

$$s(t) = \text{I} \Leftrightarrow \mu(t) = 1/2, \qquad s(t) = \text{II} \Leftrightarrow \mu(t) = -1/2.$$

As in the proof of Theorem 2, consider time instants $t_k = r_k + \epsilon/2$, with r_k the time instants such that $s(r_k) = \text{I}$ and $s(r_k^-) = \text{II}$ and write

$$\varepsilon(t_{k+1}) = \Phi_k \varepsilon(t_k) + \int_{t_k}^{t_{k+1}} \Phi(t_{k+1} - \tau, t_k) B_d \tilde{u}(\tau) d\tau$$

$$- \int_{t_k}^{t_{k+1}} \Phi(t_{k+1} - \tau, t_k) \Sigma(\tau, z, \varepsilon) d\tau,$$

with Φ_k and $\Phi(\cdot, \cdot)$ as defined in the proof of Theorem 1. Consider the Lyapunov function $V(\varepsilon) = \varepsilon' P \varepsilon$, with P as in (34), and define $V_k := V(\varepsilon(t_k))$. Following similar lines as in the proof of Theorem 1, we can write

$$V_{k+1} \leq \varrho V_k + \frac{2\|P\|\bar{\Phi}^2}{(1-\varrho)} T \int_{t_k}^{t_{k+1}} \|\Sigma(\tau, z, \varepsilon)\|^2 d\tau$$

$$+ \frac{2\|P\|\bar{\Phi}^2 \|B_d\|^2}{(1-\varrho)} \left(\int_{t_k}^{t_{k+1}} |\tilde{u}(\tau)| d\tau \right)^2 \tag{A.67}$$

with $0 < \varrho < 1$. We next proceed for a PHF load and later particularize to the other load types. Combining (A.56) and (A.67), then

$$V_{k+1} \leq \varrho V_k + \frac{2T\|P\|\bar{\Phi}^2}{1-\varrho} \gamma \int_{t_k}^{t_{k+1}} \left(\|\varepsilon_{c_4}\|^2 + \|P_H \varepsilon_l\|^2 \right) d\tau$$

$$+ \frac{2\|P\|\bar{\Phi}^2 \|B_c\|^2}{1-\varrho} \left(\int_{t_k}^{t_{k+1}} |\tilde{u}(\tau)| d\tau \right)^2. \tag{A.68}$$

The derivative along the system trajectories of the Lyapunov function is

$$\dot{V}(\varepsilon) = -\varepsilon' N \varepsilon - \tilde{\rho}(t, z_{2c_4}, \varepsilon_{c_4}) \varepsilon_{c_4} - \tilde{\delta}'(t, z_{2l}, \varepsilon_l) P_H \varepsilon_l$$

$$+ \varepsilon_{c_3} \tilde{u}(t), \tag{A.69}$$

where the matrix N is as in (A.2)–(A.3). From (A.38), (40) and (A.52) it follows that

$$\dot{V}(\varepsilon) \leq -\alpha_m \left(\|\varepsilon_4' \varepsilon_c\|^2 + \|P_H \varepsilon_l\|^2 \right) + \varepsilon_{c_3} \tilde{u}(t). \tag{A.70}$$

Recall that $\tilde{u}(t) = 0$ when the trajectory $z_1(t)$ satisfies $z_{1c_3}(t) > -V_{\text{in}}$, and also when $z_{1c3}(t) = -V_{\text{in}}$ and either (i) $z_{1c2}(t) \leq 0$ and $s(t) = \text{I}$ or (ii) $z_{1c1}(t) \geq 0$ and $s(t) = \text{II}$. If $z_{1c3} = -V_{\text{in}}$, then from (45) follows that $\varepsilon_{c_3} = z_{1c3} - z_{2c_3} < -d_3 < 0$. If $z_{1c3} = -V_{\text{in}}$ and neither condition (i) nor (ii) holds, then $\tilde{u}(t) > 0$. Consequently, we have $\varepsilon_{c_3} \tilde{u}(t) \leq 0$ and from (A.70)

$$\dot{V}(\varepsilon) \leq -\alpha_m \left(\|\varepsilon_{c_4}\|^2 + \|P_H \varepsilon_l\|^2 \right). \tag{A.71}$$

Using (A.71) in (A.68), then

$$V_{k+1} \leq \varrho V_k + c_1 \int_{t_k}^{t_{k+1}} -\dot{V}(\tau) d\tau + c_2 \left(\int_{t_k}^{t_{k+1}} |\tilde{u}(\tau)| d\tau \right)^2,$$

where $c_1 = \frac{2T\|P\|\bar{\Phi}^2}{(1-\varrho)} \frac{\gamma}{\alpha_m}$ and $c_2 = \frac{2\|P\|\bar{\Phi}^2 \|B_d\|^2}{(1-\varrho)}$. Then,

$$V_{k+1} \leq \left(\frac{\varrho + c_1}{1 + c_1} \right) V_k + \frac{c_2}{1 + c_1} \left(\int_{t_k}^{t_{k+1}} |\tilde{u}(\tau)| d\tau \right)^2, \tag{A.72}$$

where $0 < \frac{\varrho + c_1}{1 + c_1} < 1$. From (A.71) we have that $\dot{V}(\varepsilon) \leq 0$. Since $V(\varepsilon)$ is monotonically nonincreasing and bounded from below by

zero, then $V(\varepsilon(t)) \to c \geq 0$ as $t \to \infty$. Now, consider Eq. (A.69) and the fact that the four terms on the right-hand side are equal to or less than zero. From integration on both sides of Eq. (A.69) between 0 and t_k with $t_k \to \infty$ follows that

$$\int_0^\infty P_\text{I} z_{1c_2} dt < \infty \text{ with } P_\text{I} z_{1c_2} \geq 0 \quad \text{and} \tag{A.73}$$

$$-\int_0^\infty P_\text{II} z_{1c_1} dt < \infty \text{ with } P_\text{II} z_{1c_1} \leq 0, \quad \text{then} \tag{A.74}$$

$$\lim_{k \to \infty} \int_{t_k}^{t_{k+1}} P_\text{I} z_{1c_2} dt = 0, \qquad \lim_{k \to \infty} \int_{t_k}^{t_{k+1}} P_\text{II} z_{1c_1} dt = 0,$$

where $t_{k+1} - t_k = T_k \leq T$. So, according to this we have

$$\left(\int_{t_k}^{t_{k+1}} |\tilde{u}(\tau)| d\tau \right)^2 \to 0 \quad \text{as } k \to \infty. \tag{A.75}$$

Considering (A.75) and (A.72) and the fact that $V(\varepsilon)$ is monotonically nonincreasing, we can state that there exists a t_k from which the energy function evaluated in t_k, $V(\varepsilon(t_k))$, will be as small as desired. Note that for Mode III to be possible, the quantity V_k must satisfy $V_k \geq \frac{1}{2} C_1 d_3^2$ because $V_k \geq \frac{1}{2} C_1 \varepsilon_{c_3}^2(t_k)$ and $\varepsilon_{c_3} < -d_3 < 0$ if Mode III is reached. Therefore, an instant t^* exists from which the inverter will operate only in Mode I or II.

If the load is PH, then the bound on $\|\Sigma(t, z_2, \varepsilon)\|$ in (A.55) holds with $\tilde{\rho} \equiv 0$, (A.56) is replaced by $\|\Sigma(t, z_2, \varepsilon)\|^2 \leq a\|P_H \varepsilon_l\|^2$, (A.69) is replaced by $\dot{V}(\varepsilon) = -\lambda_m \|P_H \varepsilon_l\|^2 - \tilde{\delta}(t, \varepsilon_l, z_l) P_H \varepsilon_l + \varepsilon_{c_3} \tilde{u}t$, (A.70) is replaced by $\dot{V}(\varepsilon) \leq -\lambda_m \|P_H \varepsilon_l\|^2 + \varepsilon_{c_3} \tilde{u}(t)$, and (A.71) by $\|P_H \varepsilon_l\|^2 \leq -\dot{V}(\varepsilon)/\lambda_m$. The rest of the proof for a PH load follows similarly to the PHF load case. If the load is TVS, then (A.55) holds with $\tilde{\delta} \equiv 0$, (A.56) is replaced by $\|\Sigma(t, z_2, \varepsilon)\|^2 \leq \frac{(h_M - h_m)^2}{C_2^2} \|\varepsilon_4' \varepsilon_c\|^2$, (A.69) is replaced by $\dot{V}(\varepsilon) = -h_m \|\varepsilon_4' \varepsilon_c\|^2 - \tilde{\rho}(t, \varepsilon_{c_4}, z_{c_4}) \varepsilon_{c_4} + \varepsilon_{c_3} \tilde{u}(t)$, (A.70) is replaced by $\dot{V}(\varepsilon) \leq -h_m \|\varepsilon_4' \varepsilon_c\|^2 + \varepsilon_{c_3} \tilde{u}(t)$, and (A.71) by $\varepsilon_{c_4}^2 \leq -\dot{V}(\varepsilon)/h_m$. The rest of the proof for a TVS load follows similarly to the PHF load case. $\square$

References

Bacciotti, A., & Mazzi, L. (2005). An invariance principle for nonlinear switched systems. *Systems & Control Letters, 54*, 1109–1119.

Cao, D., Jiang, S., Yu, X., & Peng, F. Z. (2011). Low-cost semi-Z-source inverter for single-phase photovoltaic systems. *IEEE Transactions on Power Electronics, 26*(12), 3514–3523.

Cheng, D., Wang, J., & Hu, X. (2008). An extension of LaSalle's Invariance Principle and its application to multi-agent consensus. *IEEE Transactions on Automatic Control, 53*(7), 1765–1770.

Ćuk, Slobodan M. (1977). *Modelling, analysis, and design of switching converters*. (PhD thesis), California Institute of Technology.

De Nicoló, L., Haimovich, H., & Middleton, R.H. (2013). Continuous conduction stability conditions for semi-quasi-z-source inverters with resistive nonlinear loads. In *XV Reunión de trabajo en procesamiento de la información y control, RPIC, Bariloche, Argentina* (pp. 567–572).

Erickson, R.W., Ćuk, S., & Middlebrook, R.D. (1982). Large-signal modelling and analysis of switching regulators. In *IEEE power electronics specialists conf. PESC* (pp. 240–250).

Escobar, G., van der Schaft, A. J., & Ortega, R. (1999). A Hamiltonian viewpoint in the modeling of switching power converters. *Automatica, 35*, 445–452.

Filippov, A. F. (1988). *Differential equations with discontinuous right-hand sides*. Kluwer Academic Publishers.

Fuad, Y., de Koning, W. L., & van der Woude, J. W. (2004). On the stability of the pulse width-modulated Ćuk converter. *IEEE Transactions on Circuits and Systems—II: Express Briefs, 51*(8), 412–420.

Haimovich, H., Middleton, R.H., & De Nicoló, L. (2013). Large-signal stability conditions for semi-quasi-Z-source inverters: switched and average models. In *Proc. 52nd IEEE conf. on decision and control, Florence, Italy* (pp. 5999–6004).

Hespanha, J. (2004). Uniform stability of switched linear systems: extensions of La Salle's invariance principle. *IEEE Transactions on Automatic Control, 49*(4), 470–482.

Khalil, H. K. (2002). *Nonlinear systems* (3rd ed.). New Jersey: Prentice Hall.

Lehman, B., & Bass, R. M. (1996). Extensions of averaging theory for power electronic systems. *IEEE Transactions on Power Electronics, 11*(4), 542–553.

Liberzon, D. (2003). *Switching in systems and control*. Boston, MA: Birkhäuser.

Middlebrook, R.D., & Ćuk, S. (1976). A general unified approach to modeling switching-converter power stages. In *IEEE power electronics specialists conf. PESC* (pp. 73–86).

Peng, F. Z. (2003). Z-source inverter. *IEEE Transactions on Industry Applications*, *39*(2), 504–510.

Sanders, S. R., & Verghese, George C. (1992). Lyapunov-based control for switched power converters. *IEEE Transactions on Power Electronics*, *7*(1), 17–24.

Shen, M., & Peng, F. Z. (2008). Operation modes and characteristics of the Z-source inverter with small inductance or low power factor. *IEEE Transactions on Industrial Electronics*, *55*(1), 89–96.

Tang, Y., Xie, S., & Zhang, C. (2011). Single-phase Z-source inverter. *IEEE Transactions on Power Electronics*, *26*(12), 3869–3873.

Tanwani, A., Shim, H., & Liberzon, D. (2013). Observability for switched linear systems: Characterization and observer design. *IEEE Transactions on Automatic Control*, *58*(4), 891–904.

Wonham, W. M. (1985). *Linear multivariable control: a geometric approach* (3rd ed.). New York: Springer-Verlag.

Lisandro De Nicoló received the Electronics Engineering degree in 2012 from the Universidad Tecnológica Nacional (UTN), Argentina. He is currently working towards the Ph.D. Degree in Engineering (Electronics) at the Universidad Nacional de Rosario, Argentina, with the support of a scholarship from the Argentine Research Council (CONICET). His research interests include switched systems and power electronics converters, involving stability analysis and control strategies.

Hernan Haimovich received his Electronics Engineering degree in 2001 from the Universidad Nacional de Rosario (UNR), Argentina, and the Ph.D. degree from The University of Newcastle, Australia, in 2006. In 2006, he worked as a Research Assistant at the Centre for Complex Dynamic Systems and Control at the University of Newcastle, Australia, and later as an Argentine Research Council (CONICET) Postdoctoral Research Fellow at the UNR, Argentina. Dr. Haimovich currently holds an Investigator position from CONICET and an Adjunct Professor position at the School of Electronics Engineering, UNR. His research interests include switched and switching systems, networked control systems, and nonlinear control.

Richard H. Middleton completed his Ph.D. (1987) from the University of Newcastle, Australia. He was a Research Professor at the Hamilton Institute, The National University of Ireland, Maynooth from May 2007 till 2011 and is currently Professor at the University of Newcastle and Head of the School of Electrical Engineering and Computer Science. He has served as Program Chair (CDC 2006), CSS Vice President Membership Activities, and Vice President Conference Activities. In 2011, he was President of the IEEE Control Systems Society. He is a Fellow of IEEE and of IFAC, and his research interests include a broad range of Control Systems Theory and Applications, including Robotics, control of distributed systems and Systems Biology with applications to Parkinson's Disease and HIV Dynamics.